Karolinska Institutet, Department of Medicine
Cardiology Unit, Karolinska University Hospital
Stockholm, Sweden

Cardiac Memory Studies in Two Human Models

Liliane Wecke

Stockholm 2006

Cardiac Memory Studies in Two Human Models
by Liliane Wecke
Printed at ReproPrint AB, Stockholm
ISBN 91-7140-614-X

“You’d better start studying memory while you still have one.”

Mauricio B. Rosenbaum [1]

Contents

Abstract 6
List of original papers 7
List of abbreviations 8
Introduction 9
Cardiac cellular electrophysiology 12
Recording cardiac electricity 16
Electrocardiography (ECG) 16
Vectorcardiography (VCG) 16
Pacemaker treatment 20
Sick Sinus Syndrome 21
Hypertrophic Obstructive Cardiomyopathy (HOCM) 21
Wolff-Parkinson-White Syndrome (WPW syndrome) 22
Aims 23
Material and Methods 24
Studies I and II 24
Study III 25
Study IV 26
Study V 27
VCG analysis (Studies I, II and V) 29
ECG analysis (Studies II and III) 29
Statistical analysis 29
Results 31
Time-dependent variations (Studies I, II and V) 31
Cardiac memory development (Studies I, II and III) 31
Presence of cardiac memory after WPW ablation (Studies IV and V) 35
Cardiac memory dissipation (Studies I, IV and V) 38
Cardiac memory – good, bad or neutral (Studies II and III) 40
Summary of results 42
General discussion 43
Definition of cardiac memory 43
Cardiac memory and ventricular pacing 43
Cardiac memory and HOCM 45
Cardiac memory and the WPW syndrome 46
Methodology aspects 48
Mechanisms of cardiac memory 49
Implications 50
Limitations 52
Cardiac memory – future speculation 52
Conclusions 54
Acknowledgements 55
References 57
Appendix 62
Papers I-V

Abstract

Background

Cardiac memory is a form of electrical remodeling of the ventricles, where the T vector follows ("remembers") a previously altered QRS vector. On the electrocardiogram (ECG), it presents as T-wave inversions. It has been observed after periods of ventricular pacing, ventricular tachycardia, intermittent bundle branch block and after periods of preexcitation in patients with the Wolff-Parkinson-White (WPW) syndrome.

Aims

To study the occurrence, development and dissipation of *cardiac memory* in two human models, ventricular pacing and WPW ablation. In addition to conventional ECG analysis, the spatial vectorcardiogram (VCG) was analyzed in 3 dimensions, including T-vector loop morphology.

Studies I-II

Twenty patients who received DDD-R pacemakers due to symptomatic sinus bradycardia were followed daily for 1 week (n=6) or weekly for 5-8 weeks (n=14). A baseline ECG and VCG were recorded prior to pacemaker implantation. The patients were all paced endocardially in the right ventricle and the pacemakers were programmed to a short AV delay to achieve maximum ventricular stimulation. At each follow-up, the pacemakers were temporarily programmed to AAI mode to re-establish normal ventricular activation and an ECG and VCG were recorded. After this protocol, the 14 patients who were studied weekly had their pacemakers reprogrammed to individually optimized AV delays and, after 4-5 weeks, they were seen at one last follow-up. Repolarization changes assessed by T-vector amplitude and morphology changes were already present within 24 hours after the initiation of pacing. *Cardiac memory* was fully developed within one week and the VCG revealed a backward and upward rotation of the maximum T vector. After the cessation of ventricular pacing, *cardiac memory* disappeared within 4 weeks. When ventricular pacing was continued, *cardiac memory* was preserved in proportion to the percentage of ventricular pacing. After the abrupt termination of ventricular pacing, the prolongation of repolarization time (QTc) and changes in T-loop morphology suggested unfavorable effects on repolarization. During continuous ventricular pacing, the repolarization time decreased.

Study III

The effects of ventricular pacing on repolarization and *cardiac memory* were compared in 15 patients with hypertrophic obstructive cardiomyopathy (HOCM) and the patients from Studies I and II. A baseline ECG was recorded prior to pacemaker implantation. The HOCM patients were evaluated after 3 months of right ventricular endocardial pacing with a short AV delay. An ECG was first recorded during DDD pacing and then during sinus rhythm after pacing was temporarily switched off. T-wave inversions consistent with *cardiac memory* were observed in all HOCM patients and similar to controls. In contrast to sick sinus patients, there was no change in repolarization time in the HOCM group. Baseline myocardial structure and function thus make a difference to the repolarization response related to *cardiac memory*.

Studies IV-V

The occurrence and dissipation of *cardiac memory* after an accessory pathway ablation in WPW patients were studied retrospectively (Study IV) and prospectively (Study V). In Study IV, T-wave inversions in leads II, aVF and III were evaluated on ECGs from 125 patients ablated due to a posteroseptal (PS) accessory pathway. Within one day after ablation, 123 (98%) of the patients showed *cardiac memory* (T-wave inversions). In most patients, *cardiac memory* disappeared within 3 months. In Study V, ECGs and VCGs were used to compare the occurrence of *cardiac memory* after the ablation of PS (n=11) and left lateral (LL) (n=6) accessory pathways. *Cardiac memory* in the form of T-wave inversions on ECG was only seen in the PS group. Evaluation by VCG, however, revealed T-vector changes in the transverse plane in the LL group and vertical T-vector changes in the PS group. In 82% of the patients, *cardiac memory* disappeared within 3-4 weeks.

Conclusions

In humans, *cardiac memory* developed and reached steady state within 1 week after the onset of right ventricular endocardial pacing. After WPW ablation, *cardiac memory* was present, independent of accessory pathway site. *Cardiac memory* is probably an adaptation mechanism of the heart, involving a gradual change in repolarization when the activation sequence (depolarization) is altered. VCG including T-vector loop morphology is a useful and sensitive method for evaluating repolarization changes.

Key words: Cardiac memory, repolarization, pacing, WPW ablation

List of Original Papers

This thesis is based on the following studies, which will be referred to by their Roman numerals.

I

Wecke L, Gadler F, Linde C, Lundahl G, Rosen MR, Bergfeldt L.
Temporal characteristics of cardiac memory in humans: vectorcardiographic quantification in a model of cardiac pacing.
Heart Rhythm 2005;2:28-34

II

Wecke L, Lundahl G, Bergfeldt L.
Pacing-induced cardiac memory in the human ventricle: rapid and potentially deleterious electrophysiological remodeling.
In manuscript

III

Nowinski K, Wecke L, Gadler F, Linde C, Bergfeldt L.
Pacing-induced electrophysiological remodeling in hypertrophic obstructive cardiomyopathy – observations on cardiac memory.
Pacing Clin Electrophysiol 2005;28:561-567

IV

Aunes-Jansson M, Wecke L, Lurje L, Bergfeldt L, Edvardsson N.
T wave inversions following ablation of 125 posteroseptal accessory pathways.
Int J Cardiol 2006;106:75-81

V

Wecke L, Poçi D, Schwieler J, Johansson B, Lundahl G, Bergfeldt L.
The heart remembers preexcitation independent of pathway site – a vectorcardiographic study.
In manuscript

List of Abbreviations

AAI	Atrial single chamber pacing mode
ACE	Angiotensin converting enzyme
ACh	Acetylcholine
AP	Action potential
APD	Action potential duration
ARI	Activation-recovery interval
ARP	Absolute refractory period
AT	Activation time
ATP	Adenosine tri-phosphate
AV	Atrioventricular
Ca^{2+}	Calcium ion
Cl^{-}	Chloride ion
CI	Confidence interval
CNS	Central nervous system
Cx43	Connexin43
DC	Direct current
DDD	Dual chamber pacing mode
ECG	Electrocardiogram / Electrocardiography
HOCM	Hypertrophic obstructive cardiomyopathy
Hz	Hertz
I_{Ca}	Calcium current
I_{K}	Potassium current
I_{Na}	Sodium current
I_{to}	Transient outward current
K^{+}	Potassium ion
LBBB	Left bundle branch block
LL	Left lateral
LT	Long-term
MIDA	Myocardial Infarction Dynamic Analysis (Ortivus AB, Täby, Sweden)
ms	Millisecond
mV	Millivolt
Na^{+}	Sodium ion
PS	Posteroseptal
RBBB	Right bundle branch block
RF	Radiofrequency
RP	Refractory period
RPS	Right posteroseptal
RRP	Relative refractory period
SA	Sinoatrial
SR	Sarcoplasmic reticulum
SSS	Sick sinus syndrome
ST	Short-term
VCG	Vectorcardiogram / Vectorcardiography
VG	Ventricular gradient
VVI	Ventricular single chamber pacing mode
WPW	Wolff-Parkinson-White

Introduction

Until the 1960s, reports of T-wave negativities (inversions) on the electrocardiogram (ECG) recorded in patients in different clinical situations were mainly attributed to myocardial ischemia, even in the absence of other signs or symptoms. During the 1960s, a re-evaluation of this phenomenon began and alternative causes were considered. In 1969, Chatterjee et al. described T-wave inversions after periods of ventricular pacing [2, 3]. In the same year, transient T-wave inversions were described after repeated episodes of supraventricular tachycardia with a right bundle branch block (RBBB) configuration in a patient without any other evidence of cardiac disease (including normal coronary angiography) [4]. A few years later, T-wave inversions were also described after intermittent left bundle branch block (LBBB) [5, 6] and after periods of preexcitation in patients with the Wolff-Parkinson-White (WPW) syndrome [7].

After having been considered as possible signs of ischemia, these T-wave inversions were now regarded as some kind of curiosity. In spite of this, all the situations described above have in common a period of altered ventricular activation sequence, followed by the restitution of the normal activation pattern after a variable amount of time; Figure 1.

In addition, it was concluded back in 1969 by Chatterjee et al. that the post-pacing T-wave changes were the result of an abnormal ventricular activation sequence and were *not* due to artificial stimulation per se [3]. This was determined by stimulating the right ventricle during the absolute refractory period which did not give capture. Consequently, normal ventricular activation was preserved and there were no T-wave changes. These authors also concluded that the duration of the T-wave changes depended on the duration of the preceding ventricular pacing period [3].

T-wave inversions after intermittent LBBB were studied in 46 patients by Engel et al. They concluded that right precordial T-wave inversions may result from recent LBBB *itself*, since 17 of the patients had no evidence of coronary heart disease [5]. Interestingly, T-wave inversions during normal conduction had been taken as evidence of ischemia being the cause of previous episodes of LBBB.

Subsequently, WPW studies excluded a relationship between post-ablation T-wave changes and myocardial lesions induced by the ablation procedure. This was done by comparing patients with overt and concealed accessory pathways [8-13] and by following cardiac enzymes and echocardiographic evaluations [8, 10-13].

The topic of this thesis is therefore a phenomenon, which is characterized by transient T-wave abnormalities occurring after a period of altered ventricular activation sequence (depolarization). Furthermore, the T vector has the same direction as the vector of the previous altered QRS complex; Figure 2.

In 1982, Rosenbaum et al. found that there is an accumulation of these T-wave changes: meaning that repeated periods of pacing augmented the response which, together with the T wave "remembering" the paced QRS vector, suggested similarities between cardiac and central nervous system (CNS) memory [14]. Rosenbaum was thus the one who introduced the expression ***"cardiac memory"***, although Denes et al. in 1978 used the word "remember" when describing T-wave inversions after intermittent LBBB [6].

Experience from memory research in the CNS has served as a guide for exploring features of *cardiac memory* [15]. In parallel with memory in the CNS, Rosen et al. divided *cardiac memory* into short-term and long-term memory, although the definite time frames are not clear [15]. In the CNS, short-term memory (lasting minutes to hours) involves the modification of existing proteins, while long-term memory (lasting days to weeks) depends on new protein synthesis [16].

Cardiac memory and ventricular pacing

Studies of pacing-induced *cardiac memory* in humans published prior to those in the present thesis have included either very few patients or only occasional follow-up visits.

Rosenbaum et al. studied the effect of right ventricular pacing in 5 patients paced between 25 and 66 hours at rates of 100-120 beats/min and concluded that the T-wave changes progressed gradually and uniformly, although they did not reach steady state in any patient. The return to normal ECG took 8-38 days (4 patients) [14].

Alessandrini et al. studied the development of *cardiac memory* in 8 patients paced from the ventricle at 70-80 beats/min for 1 hour and 1 week. They found signs of *cardiac memory* only after the one-week pacing period and it persisted for at least 24 hours, which was the follow-up time after the cessation of ventricular pacing in this study [17].

Cardiac memory and the WPW syndrome

The early WPW studies, which included either a limited number of patients studied on few occasions, or various accessory pathway locations, concluded that the occurrence and persistence of post-ablation T-wave abnormalities appeared to be related both to the accessory pathway location and to the degree of preexcitation [8, 9, 13].

Kalbfleisch et al. found T-wave changes in 22 of 29 (76%) patients after the ablation of overt accessory pathways in different locations. In 7 of 13 patients studied after 3 months, the complete resolution of previous T-wave changes was observed [8]. Wood et al. found T-wave changes

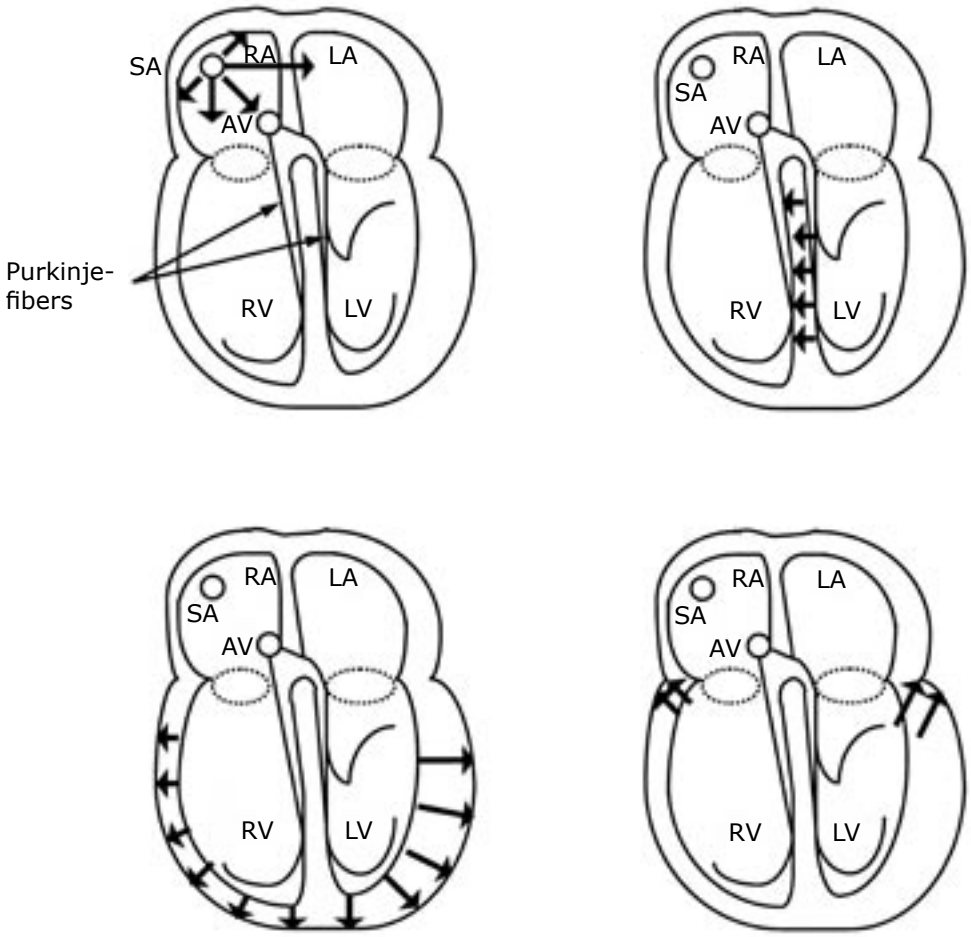

Figure 1. The normal electrical activation sequence (depolarization) of the human heart. The depolarization starts in the sinoatrial (SA) node situated in the right atrium and spreads to the left atrium. The atria are normally electrically isolated from the ventricles, apart from the atrioventricular (AV) node connecting with the His-Purkinje system. After an electrical pause, the depolarization spreads through the AV node and the bundle of His and via the Purkinje fibers throughout the ventricles. The first part of the ventricles to depolarize is the upper septum, followed by the apical wall from the endocardium to the epicardium. The last part to depolarize is the upper lateral part of the left ventricle.
LA = left atrium; LV = left ventricle; RA = right atrium; RV = right ventricle

after WPW ablation in 9 of 19 (47%) patients with overt accessory pathways in different locations. In 2 patients, T-wave changes persisted for up to 5 weeks [9].

The highest occurrence of T-wave inversions was reported in patients who had ablation of posteroseptal (PS) accessory pathways, e.g. by Poole et al. in all 7 patients studied [10, 11].

Animal studies of cardiac memory

More extensive studies of *cardiac memory* after ventricular pacing have been performed in the canine model by Professor Rosen's group at Columbia University in New York. They used both ECGs and reconstructed vectorcardiograms (VCG) in the frontal plane to study the development of *cardiac memory* in dogs paced epicardially from the left ventricle at a rate 10-15 % faster than the animals' sinus rhythm. The T-vector amplitude reached steady state after about 10 days, whereas the T-vector angle did not reach steady state until about 3 weeks of ventricular pacing. The dissipation of *cardiac memory* required ~ 7 days in dogs paced for 21-25 days and > 30 days (more than the observation time) in dogs paced for 42-52 days [18].

Mechanistic factors of *cardiac memory* have been studied in the canine pacing model. It is hypothesized that a change in the stress-strain relationship, induced by ventricular pacing, for example, activates cardiac signal systems leading to ion channel phosphorylation (short-term memory) and also to a change in gene expression and subsequently altered protein synthesis (long-term memory) [15, 19, 20].

The potassium (K^+) channel responsible for the transient outward current, I_{to}, is probably involved, since blocking of this ion channel by 4-aminopyridine abolished *cardiac memory* development in open-chest ventricular paced dogs [21], as well as in studies of epicardial and endocardial ventricular slabs [22].

It has also been shown that blocking the effect of angiotensin II (with an angiotensin converting enzyme (ACE) inhibitor *or* at the receptor level) inhibited the development of short-term *cardiac memory* in the isolated canine heart [20]. The development of long-term *cardiac memory* in intact ventricular paced dogs was delayed by the inhibition of new protein synthesis by cycloheximide [18]. *Cardiac memory* was also associ-

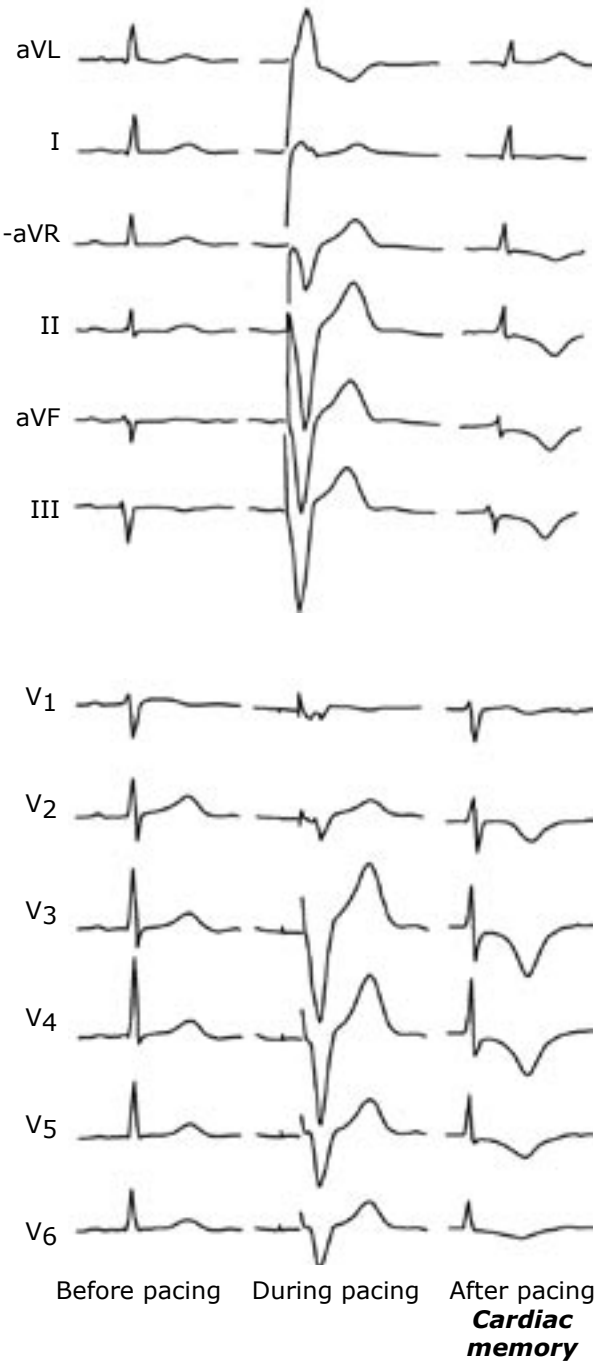

Figure 2. Pacing-induced *cardiac memory* on the 12-lead ECG. The left column shows the ECG during normal conduction prior to pacemaker implantation, the middle column the ECG *during* right ventricular endocardial pacing and the right column the ECG during normal conduction *after* 7 weeks of ventricular pacing, i.e. during *cardiac memory*. The T-wave vector during *cardiac memory* follows ("*remembers*") the paced QRS vector.
Adapted from Study I.

ated with a prolongation of the action potential duration (APD) in epicardial and endocardial cells, but not in midmyocardial cells, measured in strips of canine myocardium from controls and long-term paced dogs [18].

Background to this thesis

This was the state of knowledge when this PhD project was initiated.

The primary goal of the thesis was to study the temporal characteristics of the development and dissipation of *cardiac memory* in humans. Although it had been shown that *cardiac memory* development in the human pacing model depends on pacing duration and rate [3, 14, 17], the exact *occurrence* and the *rate* of its development and dissipation had not been defined.

Secondly, *cardiac memory* after the ablation of an accessory pathway in the WPW syndrome had been reported to last for several months in some patients [8]. However, the true occurrence of T-wave changes after the ablation of accessory pathways in different locations and the time frame for its dissipation was mainly unknown.

We hypothesized that pacing-induced *cardiac memory* would display similar general characteristics in humans compared with dogs, although the lower heart rates in humans would probably lead to the slower development of *cardiac memory* (something that proved to be wrong). We also thought that the varying clinical background would lead to a more pronounced temporal heterogeneity.

Previous studies of *cardiac memory* in humans used the 12-lead ECG to define T-wave changes, whereas a reconstructed VCG in the frontal plane was used in the dog model [18]. The VCG offers a method more easily to quantify the T-vector changes than the ECG and the VCG also provides information in all directions (if analyzed in 3 dimensions). We therefore chose to use the VCG analyzed in space for 3 of our 4 prospective studies. The study of patients paced to reduce the outflow tract obstruction (Study III) was initiated before we had begun with the VCG.

Cardiac memory has previously been regarded as a differential diagnostic problem masquerading as myocardial ischemia [5], but it is currently recognized as a variant of electrophysiological remodeling [15]. Whether it is good, bad or neutral is still an unanswered question, although pronounced repolarization changes are known to increase the risk of arrhythmias. It therefore became important to investigate this issue further, since both pacemaker treatment and WPW ablation have increased during the last decade.

The true occurrence of *cardiac memory* and the time factors for its development and dissipation are crucial factors to define in a first step. Further studies of, for example, interactions between *cardiac memory* and drugs, or attempts to modify or prevent *cardiac memory*, might then be performed.

Cardiac cellular electrophysiology

In order to appreciate the concepts related to the mechanistic discussion of *cardiac memory*, some basic electrophysiological concepts need to be explained.

Membrane potentials [23]

The cell membrane consists of a lipid bilayer which, from an electrical point of view, functions as a capacitor. The membrane potential is electro-chemical in origin and is mainly determined by the concentration of K^+ ions, which is relatively high inside the cell compared with the outside, and sodium (Na^+) ions, which have a higher concentration outside the cell. The normal resting potential of a cardiac myocyte is approximately the equilibrium potential for K^+ (-90 mV) determined by the Nernst equation, although to be exact Na^+ and chloride (Cl^-) ions should be taken into account as well:

$$\mathbf{E_K = RT/F \times \ln([K_o] / [K_i])}$$

where

E_K = the equilibrium potential for K^+ in volts (V)

R = the universal gas constant = 8.314 J/(mole K)
J= joule, K = Kelvin)

T = the absolute temperature in Kelvin (K)

F = the Faraday constant = 96485 C/mole
(C = coulomb)

K_o = K^+ concentration outside the cell
(moles per liter)

K_i = K^+ concentration inside the cell
(moles per liter)

Cardiac action potentials [23]

The cardiac action potential (AP) is the result of a complex interaction between depolarizing inward currents and repolarizing outward currents through several different ion channels. The depolarization currents mainly originate from Na^+ and calcium (Ca^{2+}) ion channels, whereas repolarization currents to a vast extent are the results of a diversity of K^+ channels.

The AP is usually divided into different phases, exemplified here by the drawing of a signal from a ventricular myocyte; Figure 3.

Phase 0: Rapid depolarization (AP upstroke): When the membrane potential reaches a level of approximately -65 mV (the threshold level), Na^+ channels suddenly open and Na^+ ions rush into the cell. This inward sodium current (I_{Na}) leads to the depolarization of the cell membrane. After just a few ms, the Na^+ channels enter the inactivated state and the channels close.

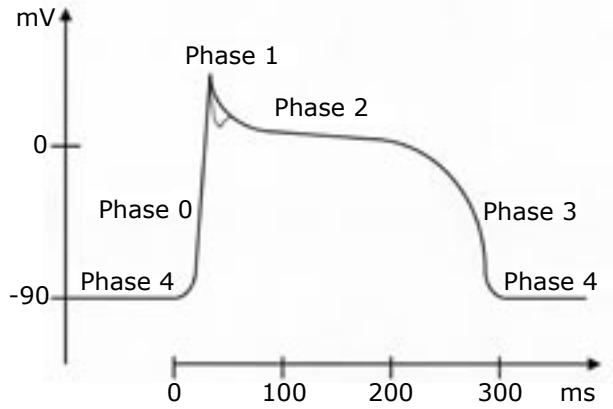

Figure 3. A typical ventricular myocardial action potential (AP) with its different phases. The broken line shows the more pronounced "notch" in epicardial cells. For details see the text.

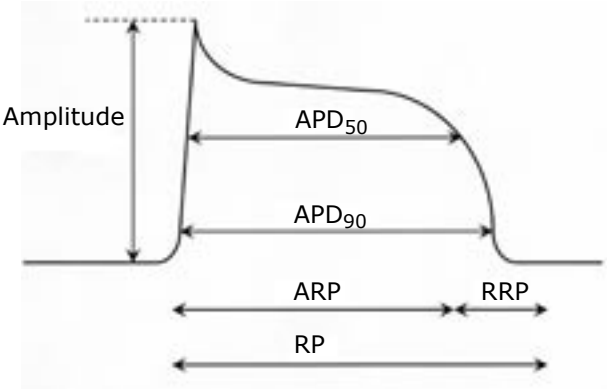

Figure 4. Action potential (AP) parameters of a typical ventricular myocardial AP. For details see the text.

Phase 1: Brief rapid repolarization: The AP upstroke (phase 0) activates K^+ channels, which give rise to the "transient outward current" I_{to}, i.e. K^+ ions leaving the cell. These channels both activate and inactivate rapidly, which results in a short repolarization seen as a notch in the AP, which is most pronounced in the epicardial cells.

Phase 2: Plateau phase: This phase is dominated by inwardly depolarizing calcium currents (I_{Ca}) and outwardly repolarizing potassium currents (I_K). The channel openings are elicited by the AP upstroke (phase 0) but have a slower activation rate and thus come into play first in phase 2. The shape of the plateau is influenced by phase 1 but is mostly determined by the balance between the inward I_{Ca} and the outward I_K currents.

This phase is the reason for myocardial APs being much longer (200-300 ms) compared with APs in nerve cells (1-2 ms).

Phase 3: Final repolarization: The depolarizing calcium currents (I_{Ca}) are inactivated and only repolarizing potassium currents (I_K) therefore remain, leading to a relatively rapid end of the plateau phase.

Phase 4: Diastolic potential: In atrial and ventricular muscle cells, the membrane potential remains relatively constant during this resting phase. The dominating current is an inwardly rectifying potassium current (I_K).

Sinoatrial (SA) and atrioventricular (AV) nodal cells have the ability for spontaneous activity (pacemaker activity). This is due to a spontaneous depolarization during phase 4, leading to the reach of the threshold potential and a subsequent AP upstroke.

AP parameters: The AP is usually characterized by some parameters; Figure 4.

AP amplitude: From the resting potential to the peak of AP depolarization.

AP duration (APD): From the onset of AP upstroke to a point at which the cell has repolarized to a defined level of its maximum, for example, APD_{50} is the APD at 50% and APD_{90} at 90% repolarization.

Absolute refractory period (ARP) and *relative refractory period (RRP):* For all excitable cells

(including cardiac cells), there is a period after each AP during which a new AP cannot be elicited, this is called the *refractory period* (RP). Cardiac cells have a much longer RP compared with other excitable cells, which lets the heart at least partially relax before the next contraction and thereby avoid tetanic contraction. The RP can be divided into the ARP during which a new AP cannot be elicited and the RRP during which an AP might be elicited if the current is larger than the normal threshold current. ARP is usually 80-85 % of the total APD.
Note that the RP might extend beyond the end of the AP, post repolarization refractoriness.

Cardiac ion channels [23]

Ion channels are built up by proteins spanning the cell membrane and forming a water-filled pore, through which ions can pass. Each channel is usually selective for one type of ion. In a simplified model, ion channels can be said to have three different states: closed, open (=activated) and inactivated. The ability of an ion channel to open or close in response to a proper stimulus is called *gating*. For the majority of the cardiac ion channels, the stimulus is a change in voltage, so-called *voltage-gated* ion channels. In the resting state, the ion channel is closed. A proper stimulus (i.e. a voltage change) will open (activate) the channel and ions will pass through it. After some time, the ion channel will become inactivated. In this state, the channel is *closed* and *cannot open* even if there is a proper stimulus. The ion channel will then return to the resting state and will subsequently again be able to open in response to a proper stimulus; Figure 5.

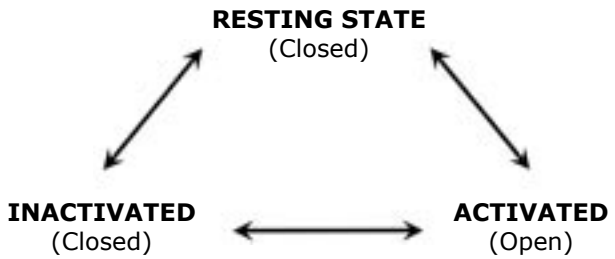

Figure 5. A simplified model of the different states of an ion channel. In the resting state, the channel is closed and no ions can pass. When a proper stimulus is applied, the channel will activate (open) and ions can pass through it. After some time, the channel will become inactivated. In this state, it is closed and cannot open, even if there is a proper stimulus.

Sodium channels (Na^+) [23]**:** Na^+ channels open rapidly (within 1 ms) when the membrane potential rises from the resting level of approximately -90 mV to -65-(-70) mV. They then rapidly inactivate almost immediately, leading to a brief influx of Na^+. This I_{Na} is responsible for the rapid upstroke (phase 0) in the AP seen in atrial and ventricular muscle cells, as well as in Purkinje cells; Figure 3. The rapid activation and inactivation make Na^+ channels important for the rapid spread of the AP throughout the myocardium.

Calcium channels (Ca^{2+}) [23-25]**:** There are two main types of Ca^{2+} channel in cardiac cells, L-type (long-lasting) and T-type (transient).
L-type Ca^{2+} channels are activated by strong depolarizations (activation threshold approximately -30 mV) and are slowly inactivated. They are present in all types of cardiac myocyte and are the main route of Ca^{2+} entry into the cells. L-type channels have three important functions:
1. To provide a sustained inward current responsible for the plateau phase (phase 2) of the AP; Figure 3.
2. To mediate the excitation-contraction coupling.
3. To generate the AP upstroke in pacemaker cells (i.e. SA and AV nodal cells).

T-type Ca^{2+} channels, on the other hand, are activated by weak depolarizations (activation threshold approximately -60 mV) and inactivate rapidly. They are mainly seen in atrial, SA and AV nodal and Purkinje cells. The T-type channels are probably involved in the generation of the pacemaker potential during phase 4.
T-type channels are present in most cardiac cells in fetal and neonate hearts and also in adult hypertrophied hearts.

Potassium channels (K^+) [23, 26-28]**:** Cardiac K^+ channels can be divided into three main categories: voltage-gated, inward rectifiers and background K^+ currents. Diversities in K^+ channels and their distribution are the main reasons for differences in APs observed during organ development, in different regions of the heart and in diseased myocardium.
The voltage-gated K^+ currents are: I_{to} (transient

outward current), I_{Kur} (ultra-rapid delayed rectifier), I_{Kr} (rapid delayed rectifier) and I_{Ks} (slow delayed rectifier). There is also one voltage-gated inward rectifier, I_{K1}.

I_{to} is responsible for the early repolarization (phase 1) of atrial and ventricular APs; Figure 3.

The three delayed rectifier K^+ currents are distinguished by different rates of activation with I_{Kur} (ultra-rapid) > I_{Kr} (rapid) > I_{Ks} (slow). They are mainly responsible for repolarization from the plateau phase in cardiac myocytes and Purkinje cells. In humans, I_{Kur} is the dominant delayed rectifier in the atrium, but it is not present in the ventricle. I_{Kr} is relatively low during the AP plateau (phase 2) but increases during phase 3, leading to the repolarization of the cell. I_{Ks} on the other hand, increases gradually during the AP plateau and remains active during phase 3.

The inward rectifier I_{K1} is active in final repolarization (phase 3) and is also a major contributor to the resting membrane potential (phase 4); Figure 3.

Other inward rectifiers are $IK_{ATP,}$ which probably activates primarily during ischemia, and $I_{KACh,}$ which is activated by acetylcholine.

Cardiac membrane pumps and ion exchangers [23]

After an AP, the ion gradients across the cell membrane have to be re-established. This is accomplished by membrane pumps, which use energy (ATP) to transport ions across the cell membrane, or by ion exchangers, which use the electrochemical gradient of one type of ions to transport another type of ions across the cell membrane. The most important are the Na^+-K^+-pump and the Na^+-Ca^{2+}-exchanger.

Excitation-contraction coupling (electro-mechanical coupling) [29]

The influx of Ca^{2+} ions during the AP plateau (phase 2) triggers a massive release of Ca^{2+} ions from the sarcoplasmic reticulum (SR), which serves as a Ca^{2+} store. The subsequent rise in intracellular Ca^{2+} concentration leads to the contraction of the cardiac myocyte via binding to contractile proteins.

Gap junctions [30-32]

Gap junctions are essentially non-selective channels that connect adjacent cardiac myocytes to each other, creating a functional syncytium. They are important for the rapid spread of the AP along cardiac cells, as well as for the spread of signal and metabolic molecules. Gap junctions are concentrated at the end of a typical cardiac myocyte but are also present all along the surface of the cell, creating a three-dimensional syncytium.

Gap junctions are built up by proteins called connexins, where connexin43 (Cx43) is the most important in the human heart. Six connexins form a connexon ("hemi-channel") and two connexons from adjacent cells dock to form a gap junction channel. The distribution of gap junctions shows regional differences in the heart and there are also differences in distribution in the fetal and young myocardium. The distribution and expression of connexins may be changed by pathological conditions, resulting in a pattern resembling the fetal or young heart. The conduction of gap junctions can also be modulated by the phosphorylation of Cx43.

Propagation [33]

When an AP is elicited, the depolarization spreads to surrounding cells. The propagation throughout the myocardium depends on the balance between the depolarizing current (current source) and the current needed to depolarize adjacent resting cells (current sink) and also on the ability of the current to move through gap junctions.

Diversity of cardiac cells [26, 28, 34]

The AP waveform varies in different regions of the human heart, which influences excitation-contraction coupling, propagation and also the heterogeneity of repolarization. The difference in AP is mainly due to different expressions of voltage-gated K^+ channels.

Furthermore, cardiac disease often leads to changes in the distribution or properties of voltage-gated K^+ channels and subsequently to changes in the AP, which may in turn create a substrate for arrhythmias.

There are also local differences in APs within the myocardium, with ventricular endocardial cells having a longer APD without the phase 1 notch, compared with the epicardial cells with a shorter APD and a pronounced phase 1 notch. The midmyocardial M-cells have an even longer APD, which also has the ability to

prolong more than the APD of endocardial and epicardial cells. However, when the cells form a continuous syncytium, such as in the normal myocardium, they interact electrotonically and the differences are smoothed out.

Recording cardiac electricity [35]

Cardiac electricity was first recorded in the frog heart in 1856 by Kolliker and Muller. The first human ECG was recorded in 1887 by Waller, who also suggested that the electromotive force of the heart could be represented by a single dipole. In 1913, Einthoven et al. introduced the concept of the mean electrical axis of the heart, represented by a vector. The first publication describing a VCG was published as early as 1914 by Williams.

Electrocardiography (ECG)

The spread of electrical activation through the myocardium can be recorded on the surface of the body as changes in electrical potentials, the ECG. The relationship between the different parts of the ECG and a typical ventricular action potential is shown in Figure 6.

The QT interval is used as an ECG measure of the repolarization time of the ventricles, although it represents both depolarization and repolarization. Another measurement of repolarization time is the activation-recovery interval (ARI) [36], see Figure 6.

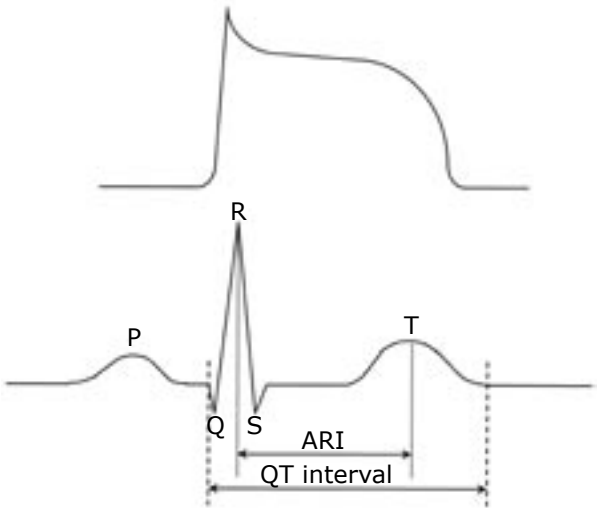

Figure 6. The relationship between the ECG and a typical ventricular action potential. The QRS complex depicts the depolarization of ventricular myocardial cells and the T wave their subsequent repolarization. The QT interval is a measure of ventricular repolarization time. Sometimes the activation-recovery interval (ARI) is used to represent the repolarization time.

Vectorcardiography (VCG)

Dipoles and vectors [37, 38]

The spread of electrical potentials between heart cells during each cardiac cycle produces an electrical field in the surrounding tissues extending to the body surface. The heart could therefore be regarded as a generator situated in a volume conductor, the body. The electrical potential, V_P, at any point, P, in a volume conductor could be calculated as:

$V_P = \mu \cos \theta / d^2$

where μ is the dipole moment, which is the product of the charge and the length of the dipole, d is the distance from point P to the center of the di-

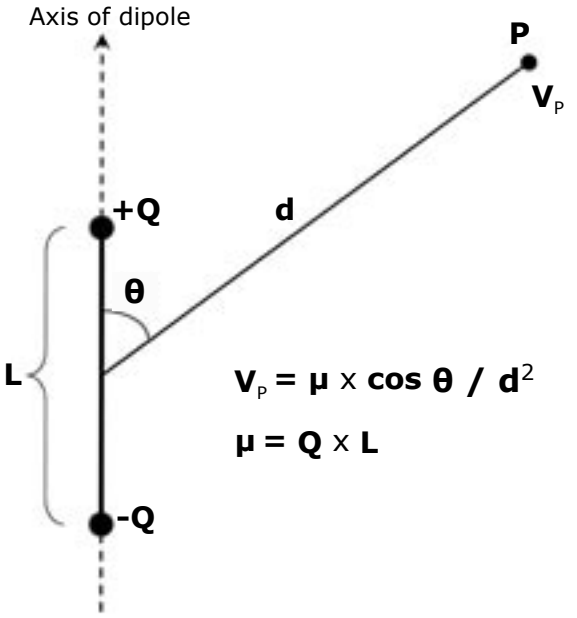

Figure 7. In a volume conductor, the electrical potential, V_P, at the point, P, at distance, d, from a dipole could be calculated as:

$V_P = \mu \cos \theta / d^2$

where

μ = the dipole moment, which is the product of the charge (Q) and the length (L) of the dipole

θ = the angle between the dipole axis and the line to point P

d = the distance from point P to the center of the dipole

pole and θ is the angle between the dipole axis and the line to a distant point, P; Figure 7.
The above-mentioned features and relationships apply to the ideal situation where:

1. The dipole is situated in an infinitely large volume conductor. The heart is, however, fairly large compared with the body and it is also located eccentrically in the thorax. The human body is also finite in size with an irregular limiting boundary surface.
2. The volume conductor is homogeneous and isotropic. However, the human body is inhomogeneous and anisotropic, with different electrical conductivities of various tissues. The blood, however, which has low electrical resistance and consequently a short-circuiting effect within the heart cavities, probably leads to the unification of electrical activity and the heart could therefore be regarded as a single dipole.

For each moment in the cardiac cycle, the electromotive force can be represented by a vector, depicted as an arrow. The length of the vector represents the magnitude and the direction depicts the spatial direction of the electromotive force. The origin of the vector is assumed to be in the center of the heart mass and remains in this position throughout the cardiac cycle. The arrowhead forms continuous loops in 3 dimensions during the cardiac cycle, the spatial VCG. The spatial VCG consists of 3 consecutive loops, the P loop representing *atrial depolarization*, the QRS loop representing *ventricular depolarization* and the T loop representing *ventricular repolarization*. For practical reasons, the VCG is often displayed as projections on 3 orthogonal planes, the horizontal / transverse plane, the frontal plane and the left or right sagittal plane. Nor is there any general agreement about whether the left or right sagittal plane should be used, or which direction should be positive or negative on each axis. In this thesis, we have used the definitions utilized by the MIDA system (see below), which are the *left* sagittal plane and axis directions as depicted in Figures 8 and 13.

Lead systems

For recording of the vector representing the resultant cardiac electromotive force, a system of leads measuring the vector components in 3 mutually perpendicular directions is needed. There are more than 30 different lead systems, although only a few of them are in practical use, and as yet there is *no* international standard.
The 8-electrode (one ground electrode) system according to Frank is the most commonly used, since it offers a good compromise between accuracy of measurement and simplicity of use [39].
The Frank lead system utilizes 5 electrodes at the level of the fifth intercostal space, which is where the origin of the heart dipole is assumed to be situated. In addition, one electrode is placed on the back of the neck, one on the left leg and a ground electrode on the right leg, see Figure 8. The values of the X, Y and Z leads are calculated from the electrodes according to the following equations:

$$X = 0.610 \times A + 0.171 \times C - 0.781 \times I$$
$$Y = 0.655 \times F + 0.345 \times M - 1.000 \times H$$
$$Z = 0.133 \times A + 0.736 \times M - 0.264 \times I - 0.374 \times E - 0.231 \times C$$

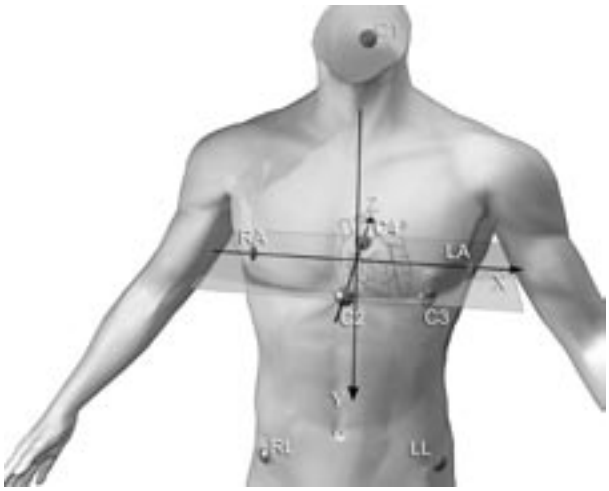

Figure 8. The MIDA system utilizes 8 electrodes positioned according to the Frank orthogonal lead system (X, Y, Z). The letters inside brackets correspond to the equations in the text.
Five electrodes are positioned at the level of the fifth intercostal space:
C2 (E): on the front at the midline
C4 (M): on the back at the midline
RA (I): right midaxillary line
LA (A): left midaxillary line
C3 (C): between C2 and LA at a 45º angle

The 3 other electrodes are positioned:
C1 (H): on the back of the neck
LL (F): left hip
RL: right hip (ground electrode)

Parameters

The VCG is a spatial (3 dimensions) measurement which also has a "fourth dimension", i.e. time, and can be analyzed according to several parameters:

- The magnitude and direction of the maximum vector in space (P, QRS or T vector): expressed here as amplitude, azimuth and elevation; Figures 9 and 10.
- The loop configuration (P, QRS or T loop): in this thesis, the T-loop configuration is analyzed using the parameters Tavplan, Tegenv and Tarea; Figures 11 and 12.
- QRS-T angle: calculated as the difference between maximum QRS and T vectors - not analyzed in this thesis.
- Direction and speed of the inscription of the loop (P, QRS or T loop) - not analyzed in this thesis.

The angles of the maximum vector in space can be expressed as *azimuth* and *elevation*.

Azimuth: The angle in the transverse plane, defined as zero when the vector is pointing to the left. Forward vector directions are defined as 0-180° and backward vector directions as 0-(-180)°; Figure 9.

Elevation: The angle between the vector and an axis perpendicular to the transverse plane, zero being the vector pointing downwards; Figure 10.

The configuration of the T loop can be expressed by the parameters *Tavplan*, *Tegenv* and *Tarea*.

Tavplan: A measure of the bulginess of the loop, defined as the mean distance from the preferential plane for the sample values of the T loop. The sample values are all points in space and time representing the circumference of the T loop. A higher value of Tavplan means a more bulgy loop, which is a sign of increased repolarization heterogeneity [40, 41] ; Figure 11.

Tegenv: A measure of the form and symmetry of the T loop. Considering the sample values of the T loop as mass points, the matrix of inertia can be defined [42]. Tegenv is calculated as the quotient between the two highest eigenvalues (≈diameters) of the matrix of the inertia; Tegenv = $(d1/d2)^2$, where d1 > d2. For the special case of a circle, Tegenv = 1. A higher Tegenv stands for a more elongated loop. A decrease in Tegenv (more circular T loop) is associated with increased repolarization heterogeneity [43, 44]; Figure 12.

In simplified terms, the T loop can be regarded as a "rubber band" in space. The longest axis around which it can most easily rotate should be found, this is d1. Then d2 is the axis perpendicular to d1 allowing the easiest rotation. The third perpendicular axis, d3, is normally close to zero and can therefore be ignored.

Tarea: The "three-dimensional" area between the curve and the baseline from the QRS end (J point)

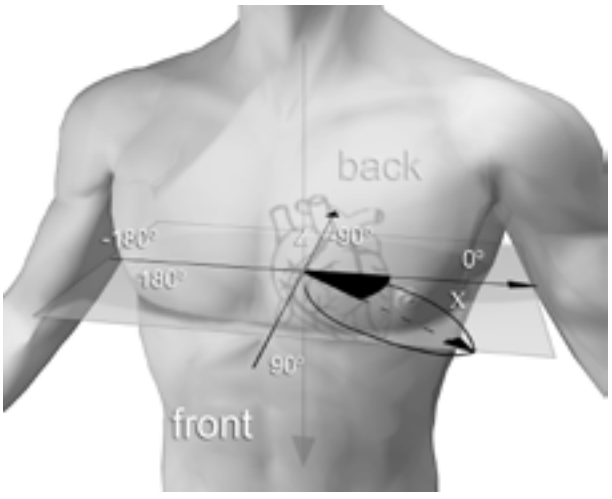

Figure 9. Vectorcardiogram (VCG) of the T-vector loop with its maximum vector in space.
T azimuth is the angle in the transverse plane (X-Z plane), defined as zero when the vector is pointing to the left. Forward vector directions are defined as 0-180° and backward vector directions as 0-(-180)°.

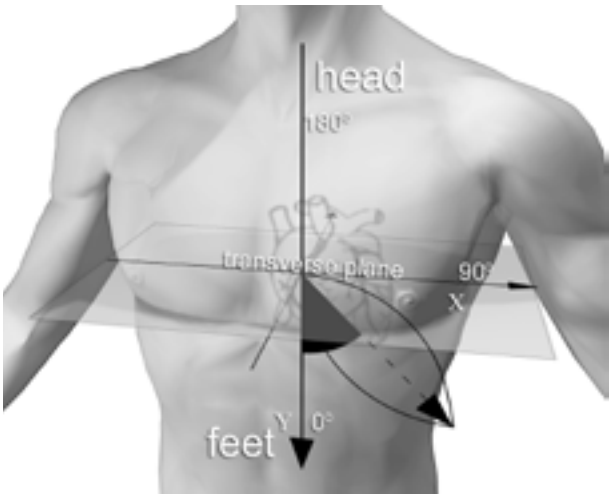

Figure 10. Vectorcardiogram (VCG) of the T-vector loop with its maximum vector in space.
T elevation is the angle between the vector and an axis (Y-axis) perpendicular to the transverse plane, defined as zero when pointing downwards and 180° pointing in the cranial direction.

to the T end in the Frank leads X, Y and Z, calculated as $(Tx^2 + Ty^2 + Tz^2)^{½}$.

Since *cardiac memory* is a variant of repolarization changes in the ventricles, this thesis focuses on the T loop. Previous studies of *cardiac memory* have used the ECG (mainly humans) or VCG (mainly dogs) analyzed in one or two planes (frontal and horizontal planes). However, the cardiac vector is a three-dimensional phenomenon and we therefore chose to analyze the vector in all 3 dimensions using the spatial maximum T-vector amplitude, azimuth and elevation. If analysis is performed in only one plane information could be lost or misinterpreted. For example, the maximum spatial vector amplitude does not always coincide with the maximum vector amplitude in one plane, since the latter is a projection of the former onto the actual plane.

Analysis of the T-vector loop *morphology* presumably provides more information about the repolarization process than analysis of only the *maximum* T vector in space. Although the concept is fairly new, previous studies have shown an association between increased repolarization heterogeneity or QT dispersion and increased values of Tavplan (more "bulgy" loop), as well as decreased values of Tegenv (more circular loop) [40, 41, 43, 44].

The human T-vector loop is normally elongated or narrow in shape, with a smooth contour, and is mainly situated in one preferential plane. The initial "departing" phase (efferent limb) is inscribed more slowly than the "returning" phase (afferent limb) and the maximum T vector is usually directed to the left, inferiorly and anteriorly; Figure 13.

The MIDA (Myocardial Infarction Dynamic Analysis) system

For recordings of VCGs, a MIDA 1000 system (Myocardial Infarction Dynamic Analysis, Ortivus AB, Täby, Sweden) was used. This system utilizes 8 electrodes positioned according to the Frank orthogonal lead system (X, Y and Z); Figure 8. The sampling frequency for each electrode is 500 Hz. All ECG complexes are classified according to morphology and presented in a table on the MIDA monitor. The operator (technician, research nurse) confirms the correctness of the reference class chosen by the system (usually the most prevalent QRST complex) and the registration can then begin. QRST complexes which conform to the reference class are then averaged over a programmable time period (minimum 2 seconds, maximum 4 minutes). The result is presented in the transverse, frontal and left sagittal planes for each loop (P, QRS and T); Figure 13.

The analysis of loop parameters, maximum vector amplitude, azimuth and elevation, as well as Tavplan, Tegenv and Tarea, was performed off-line.

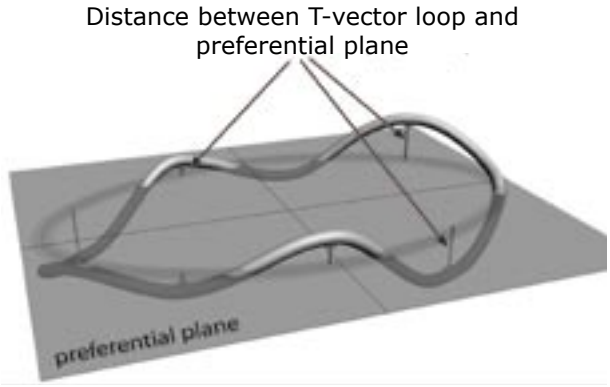

Figure 11. Tavplan is the mean distance between the T-vector loop and its preferential plane ("the bulginess of the loop"); (μV).
The darker shade of gray is below the preferential plane and the brighter shade is above it.
See the text for details.

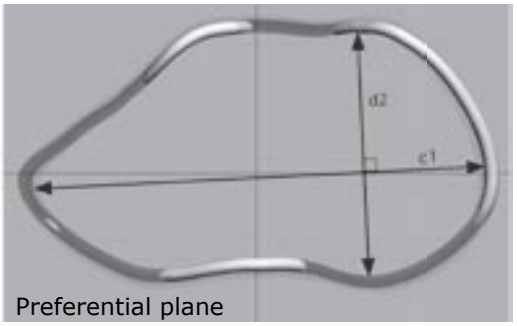

Figure 12. Tegenv is the quotient of the two highest eigenvalues (d1 & d2; ~diameters) of the T-vector loop ("the form of the loop"); (unitless).
The darker shade of gray is below the preferential plane and the brighter shade is above it.
See the text for details.

Pacemaker treatment

The first permanent pacemaker implantation was performed in 1958 at Karolinska University Hospital in Solna, Sweden. This device stimulated the ventricle at a fixed rate, so called V00-mode (see below). Since then, the technology has experienced tremendous development and current pacemakers are multi-programmable devices, often with more than one stimulation and sensing site. Furthermore, the indications for pacemaker treatment have broadened from bradycardia therapy to the treatment of outflow tract obstruction in some patients with Hypertrophic Obstructive Cardiomyopathy (HOCM) and resynchronization therapy (biventricular pacing) in heart failure patients.

A three-letter code was introduced in 1974 to describe the basic functions of a pacemaker system and, after the last revision in 2001, it now comprises five letters. The first letter refers to the chamber or chambers where stimulation occurs and the second letter to where sensing occurs. The letters that are used are A = atrium, V = ventricle, D = dual chamber (both A and V), S = single chamber (A or V), 0 = none. The third position describes how the pacemaker responds to a sensed event,

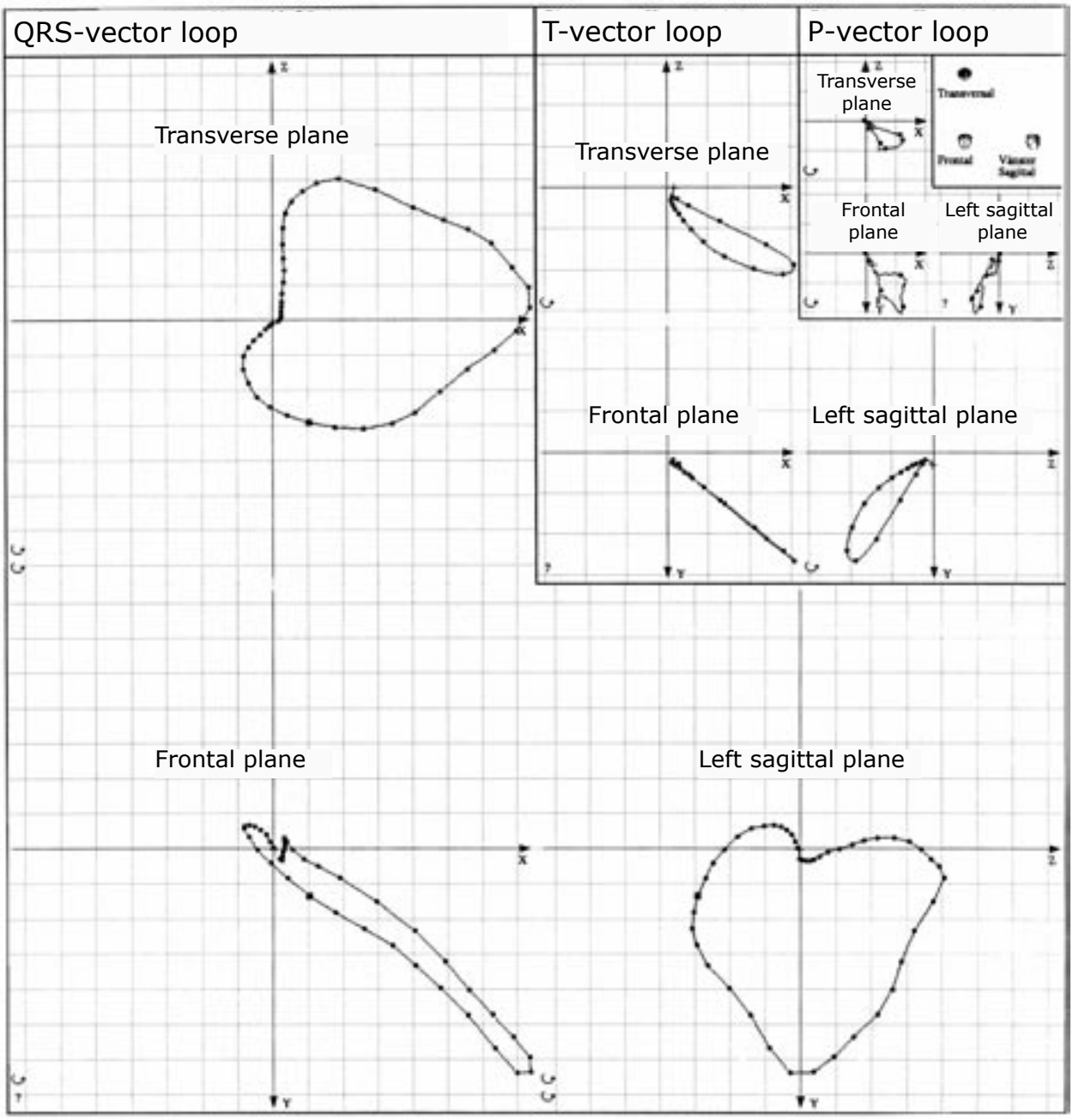

Figure 13. The MIDA system presents the result in the transverse, frontal and left sagittal planes for each loop (P, QRS and T). VCG from a healthy control.

I = inhibiting, T = triggering, D = both I and T, 0 = no sensing function. An "R" in the fourth position indicates that the pacemaker is capable of rate modulation, i.e. automatic heart rate increase. The fifth position indicates whether there is multisite pacing in the atrium (A), ventricle (V) or both (D).

Sick Sinus Syndrome

Sick Sinus Syndrome (SSS) is probably due to the aging and degeneration of the sinus node (SA node). It is a common cause of symptomatic arrhythmias in the form of sinus bradycardia, sinus arrest or alternating bradycardia and atrial tachyarrhythmias in the elderly. Patients with symptoms of syncope or presyncope and documented sinus bradycardia or a prolonged (≥ 800 ms) corrected sinus node recovery time (CSNRT) measured during invasive electrophysiological testing should receive permanent pacemaker treatment.

Hypertrophic Obstructive Cardiomyopathy (HOCM)

HOCM is a special form of hypertrophic cardiomyopathy with a hypertrophied interventricular septum and abnormal function of the anterior mitral leaflet, leading to left ventricular outflow tract obstruction. The disease is often genetically determined and carries an increased risk of sudden cardiac death, probably due to arrhythmia. Histologically, there is a disorganization of muscle bundles with abnormalities in the cell-to-cell arrangement, fibrosis and disorganization of myofibrils within myocytes.
Treatment is pharmacological with beta blockers and/or calcium antagonists, sometimes combined with myectomy or alcohol ablation to reduce the thickness of the interventricular septum, or DDD pacing with a short AV delay to diminish the outflow tract obstruction.

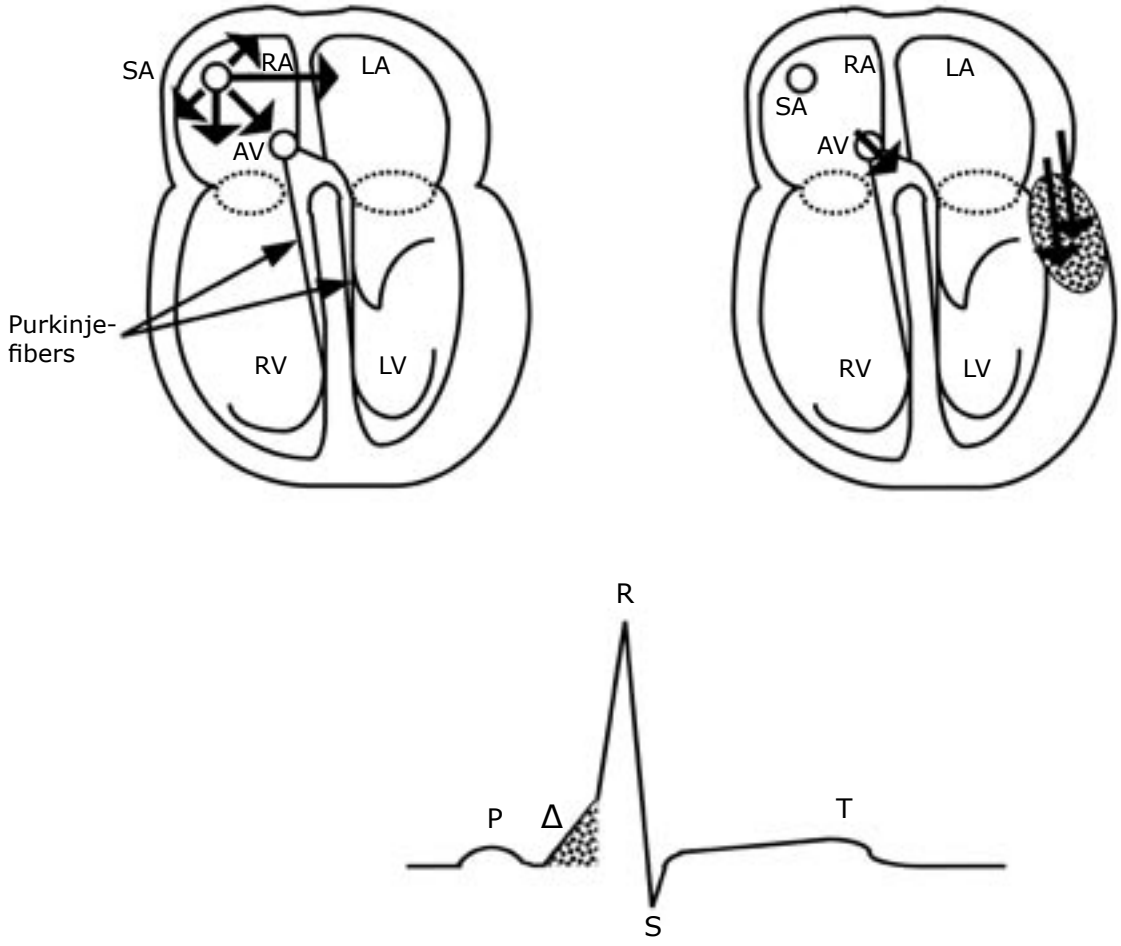

Figure 14. In the WPW syndrome with a left lateral (LL) accessory pathway, the left ventricle starts to depolarize (preexcites) before initiation of the normal depolarization of the septum through the His-Purkinje fibers. This can be seen as the Δ = delta wave on the ECG.

Wolff-Parkinson-White Syndrome (WPW syndrome)

The original definition of the WPW syndrome is a combination of episodes of supraventricular tachycardia and ECG with ventricular preexcitation (=delta wave on ECG). It is a congenital disorder with at least one accessory atrioventricular (AV) pathway, somewhere along the AV annuli. The most common location is the left free wall (50-60%). The classic WPW syndrome has an accessory pathway with antegrade conduction (atrium to ventricle) responsible for the delta wave on the ECG during sinus rhythm and retrograde conduction (ventricle to atrium) giving rise to orthodromic AV reciprocating tachycardia. Some patients have an accessory pathway with only retrograde conduction, leading to orthodromic tachycardia but no delta wave during sinus rhythm. This is often referred to as WPW syndrome with a concealed accessory pathway. Very few patients only have antegrade accessory pathway conduction.

Conduction over an accessory pathway is relatively rate *independent* (non-decremental) compared with the normal (decremental) AV conduction. This leads to a potential risk of sudden cardiac death if atrial fibrillation is conducted to the ventricles through the accessory pathway, giving rise to a rapid ventricular response which can degenerate into ventricular fibrillation.

Nowadays, WPW syndrome can be cured by radiofrequency (RF) ablation of the accessory pathway using catheterization techniques; Figure 14.

Aims

The main goal for this thesis was to study the occurrence, development and dissipation (resolution) of *cardiac memory* in two different human models (ventricular pacing and WPW syndrome), using electrocardiography (ECG) and vectorcardiography (VCG). The sequence below represents the order chosen for presentation rather than the temporal process of the PhD project, which followed different parallel tracks.

In more detail:

- To define the temporal characteristics of the development of pacing-induced *cardiac memory* and shed some light on its dissipation (Study I)
- To describe the sequence of appearance of repolarization changes related to pacing-induced *cardiac memory* as reflected by different ECG and VCG parameters (Study II)
- To shed some light on possible positive and negative effects on ventricular repolarization as a consequence of pacing-induced *cardiac memory* (Studies II & III)
- To compare pacing-induced *cardiac memory* in patients with and without (controls) hypertrophic obstructive cardiomyopathy (HOCM) (Study III)
- To study the occurrence of and time frame for the dissipation of *cardiac memory* after WPW ablation (Studies IV & V)
- To compare the incidence and characteristics of *cardiac memory* after WPW ablation of posteroseptal and left lateral accessory pathways (Study V)

Material and Methods

Two different models were used to study *cardiac memory* in humans, endocardial right ventricular pacing and the ablation of accessory pathways in patients with the WPW syndrome. The two models are complementary. The pacing model (Studies I-III) provides an opportunity to study *cardiac memory development,* as well as its *dissipation*, since pacemaker stimulation can be set at on or off. Translational research is possible because both experimental *in vitro* and *in vivo* models are available.

In contrast, the treatment of WPW patients (Studies IV-V) provides a model that is unique to humans. Compared with the pacing model, this is a completely different situation, with an abnormal activation pattern that is congenital, and after ablation a normal pattern is acquired. However, only *cardiac memory dissipation* can be studied in this model, but the "memory" has been induced during a period of years and even decades.

Studies I and II

The time frame for the development of pacing-induced *cardiac memory* and related repolarization changes was studied in a group of patients with only mild structural heart disease. In addition, some data on the dissipation of *cardiac memory* was also achieved.

Patients

These studies were conducted on two series of patients who received DDD-R pacemakers due to symptomatic sinus bradycardia. They had no or only mild structural heart disease and their standard 12-lead ECGs were classified as normal or with only minor changes.

The first series of patients who were enrolled are referred to as the "long-term" (LT) patients. This series consisted of 14 patients (8 women, mean age 71 ± 13 years, range 41-84 years), who were followed weekly for 5-8 weeks after pacemaker implantation. Since *cardiac memory* development turned out to be much faster than anticipated, a second series of patients was included. These "short-term" (ST) patients were followed daily during the first week after pacemaker implantation and the series consisted of 6 patients (4 men, mean age 58 ± 18 years, range 27-79 years). Baseline characteristics for the study patients are presented in Table 1 and detailed data on the actual pacemaker programming can be found in Appendix 1.

A control group of 10 healthy individuals (5 women), mean age 41 ± 7 years (range 28-51), was included to assess the time-dependent variability in T-vector angles. In this group, VCGs were recorded twice with one week's interval.

Protocols

Within 24 hours prior to pacemaker implantation, a 12-lead ECG and a VCG were recorded during sinus rhythm. All patients received a DDD-R pacemaker connected to leads in the right atrium and the right ventricular apex. Within 4 hours after the implantation, the pacemaker was programmed to DDD or DDD-R mode with a short AV delay to ascertain maximum ventricular stimulation. The patients were seen the day after pacemaker implantation and then weekly for 5-8 weeks (LT patients) or daily for one week (ST patients). At each visit, the pacemaker was temporarily programmed to AAI mode to re-establish normal ventricular activation. An ECG and VCG were recorded and the pacemaker log was reviewed for the percentage of ventricular paced cardiac cycles since the last follow-up. This first phase of the protocol provided information about the development of pacing-induced *cardiac memory*. During the second phase, the pacemaker was programmed to an AV delay optimized for each individual patient to reduce the amount of ventricular pacing. To obtain information on *cardiac memory* dissipation, the LT patients were then seen once more after 4-5 weeks. The same procedure as

during the first part of the protocol was used, with ECG and VCG recordings performed during AAI pacing.

Analyses in Study I

The ECGs were analyzed qualitatively to define the presence or absence of *cardiac memory* (T-wave inversions).
The VCGs were analyzed quantitatively (maximum T-vector azimuth and elevation) to define the temporal characteristics of *cardiac memory* development and dissipation.

Analyses in Study II

The ECGs were analyzed quantitatively during normal activation and during ventricular pacing and the QRS, QT, QTc, JT and JTc intervals were assessed, together with QT and JT dispersion.
The VCGs were further analyzed quantitatively adding the parameter maximum T-vector amplitude and the T-vector loop morphology parameters Tavplan, Tegenv and Tarea.

Study III

The effect of ventricular pacing on repolarization and *cardiac memory* in HOCM patients was compared with the effects in patients without HOCM.

Patients

The HOCM group consisted of 15 patients (9 men) with a mean age of 66 ± 11 years (range 48-89 years). They were accepted for pacemaker therapy designed to reduce the left ventricular outflow tract obstruction because of significant symptoms despite optimal pharmacological treatment. For a comparison of ECG parameters

Table 1. Clinical characteristics of the 14 long-term (LT) and 6 short-term (ST) study patients paced because of symptomatic sinus bradycardia.

Patient	Age/Gender	Cardiovascular disorders	Cardioactive drugs
LT01	81/M	HT, stroke, CAD, AS	None
LT02	77/F	HT, stroke	Ca-antagonist
LT03	77/M	None	None
LT04	41/F	None	None
LT05	58/M	None	None
LT06	55/F	HT	BB
LT07	82/F	HT, stroke, CAD, CHF	Ca-antagonist
LT08	60/M	PAF, TIA, Churg-Strauss	Sotalol
LT10	67/M	None	None
LT11	80/M	HT, PAF, AR	Sotalol, digoxin, doxazosin, ACEI
LT12	84/F	PAF, CHF	BB (from week 1)
LT13	82/F	HT, CAD, CHF	ACEI, TCA
LT14	78/F	None	BB
LT15	70/F	PAF	BB
ST01	54/M	None	None
ST02	72/F	HT, PVD, PAF	BB, Ca-antagonist, ARB
ST03	63/F	None	None
ST04	79/M	None	None
ST05	54/M	HT, CAD, stroke	BB, ACEI, Ca-antagonist
ST06	27/M	None	None

ACEI = angiotensin converting enzyme inhibitor; AR = aortic regurgitation; ARB = angiotensin II type 1 receptor blocker; AS = aortic stenosis; BB = beta blocker; CAD = coronary artery disease; CHF = congestive heart failure; HT = hypertension; PAF = paroxysmal atrial fibrillation; PVD = peripheral vascular disease; TCA = tricyclic antidepressants; TIA = transitory ischemic attack
Reprinted from Study I with permission from the publisher.

recorded *during* ventricular pacing and post-pacing sinus rhythm (after abruptly stopping pacing), 30 more HOCM patients were added. They had received their pacemaker systems before the present study was started and were not studied at baseline.
The control group was identical with the 14 LT patients from Studies I and II (see above).

Protocol

Before pacemaker implantation, a standard 12-lead ECG was recorded in both groups. All patients received a DDD/DDD-R pacemaker connected to leads in the right atrium and right ventricular apex. Within one day after implantation, the pacemakers were programmed to a short AV delay to achieve maximum ventricular preexcitation.
The HOCM group (n=15) was then evaluated after ≥ 3 months of DDD pacing. An ECG was first recorded during DDD pacing and then during sinus rhythm after pacing was temporarily switched off.
The control group (n=14) was evaluated as described above.

Analyses

The ECGs were analyzed qualitatively as well as quantitatively. *Cardiac memory* was defined as the presence of negative T waves in the inferior leads (II, aVF, III) during normal AV conduction (sinus rhythm or AAI pacing) tracking the vector of the previously paced QRS complex. The ECG parameters RR, QRS, QT, QTc, JT and JTc intervals were assessed, as well as QT, QTc, JT and JTc dispersion.
For the HOCM group (n=15), as well as for the extended HOCM group (n=45), ECG recordings *during* ventricular pacing after the development of *cardiac memory* were analyzed quantitatively and compared with the post-pacing sinus rhythm.

Study IV

The *occurrence* and *dissipation* of *cardiac memory* after the ablation of an overt accessory pathway in WPW patients were assessed in this retrospective study. According to previous studies, ECG signs of *cardiac memory* appeared most consistently after the ablation of PS accessory pathways, a location that is not very common. For the purpose of this study, we needed a large number of patients with an accessory pathway in a location known to show signs of cardiac memory and we therefore chose to perform a retrospective study.

Patients

Records from all patients with an overt PS accessory pathway who underwent successful ablation at Karolinska and Sahlgrenska University Hospitals between 1991 and 2001 (n=155) were scrutinized. Patients with bundle branch block, a pacemaker, more than one overt accessory pathway, recurrence of the accessory pathway conduction, pericarditis, ischemic heart disease and ECGs not available were excluded (n=30). The remaining 125 patients (70 men) had a mean age of 35 ± 15 years, range 8-76 years. In 119 (95%) patients, the WPW syndrome was the only cardiovascular disorder and 94 (75%) had no concomitant disease. The clinical characteristics of the study group are presented in Table 2.

Protocol

Medical records were examined retrospectively and all available ECGs up to one year after the ablation procedure were evaluated by two physicians jointly.

Analyses

The ECGs were analyzed qualitatively. Since previous studies had shown that ECG changes (T-wave inversions) after the ablation of overt PS accessory pathways are mainly seen in the inferior leads II, aVF and III [8, 10, 11, 13], the ECG analysis focused on these leads.
The QRS complexes *before ablation* were classified as R/S>1, R/S<1 or R/S=1 according to the areas above and below the isoelectric baseline. The delta-wave polarity was classified as positive (+), negative (-), biphasic (+/- or -/+) or isoelectric (0). The T-wave polarity *after* ablation was classified as positive (+), negative (-), biphasic (+/- or -/+) or isoelectric (0) and was compared with the dominant QRS force and the delta wave prior to ablation in *each* of the inferior leads.
In order to estimate the degree of preexcitation, the QRS width (QRS duration including the

delta wave) in the inferior leads was measured prior to and immediately after the ablation procedure and the difference was calculated. The QRS duration prior to ablation was also categorized, according to previous studies [8, 13], as ≤ 100 ms or >100 ms and compared with post-ablation T-wave changes.

Study V

The occurrence of *cardiac memory* after the successful RF ablation of overt accessory pathways in different locations was assessed in this prospective study at the Karolinska and Sahlgrenska University Hospitals. Previous studies had shown that ECG signs of *cardiac memory* occured more frequently after the successful ablation of PS than after left lateral (LL) accessory pathways. We hypothesized that this difference was due to limitations in the ECG technique to detect repolarization changes in all directions and we therefore used VCG to study the occurrence of cardiac memory after the successful ablation of overt PS compared with LL accessory pathways. Patients ablated due to a concealed accessory pathway served as an internal control group.

Table 2. Clinical characteristics of 125 patients with a successful ablation of an overt posteroseptal accessory pathway, n (%).

Mean age ± SD (range)	35 ± 15	(8-76 years)
Gender (F/M)	55 / 70	(44% / 56%)
Concomitant cardiovascular disorders		
None	119	(95%)
Hypertension	4	(3%)
DCM	1	
VSD	1	
Echocardiography		
Normal	78	(62%)
Valvular disease	5	(4%)
LVH	2	
VSD / ASD	1 / 2	
DCM	1	
Minor abnormalities	7	(6%)
N/A	29	(23%)
Documented arrhythmia		
OT	66	(53%)
AF / AFl	43 / 2	(34% / 2%)
Preexcited AF / AFl	36 / 0	(29% / -)
AT	11	(9%)
VF	5	(4%)
None	31	(25%)
Arrhythmia history	**Yes / No / NA**	
CPR	5 / 120 / 0	(4/96/0%)
Syncope	23 / 96 / 6	(18/77/5%)
Presyncope	38 / 65 / 22	(30/52/18%)
Prior ablation attempt	23	(18%)
Prior arrhythmia surgery	2	(2%)

AF = Atrial fibrillation; AFl = Atrial flutter; ASD = Atrial septum defect; AT = Antedromic tachycardia; CPR = Cardio-pulmonary resuscitation; DCM = Dilated cardiomyopathy; LVH = Left ventricular hypertrophy; OT = Orthodromic tachycardia; VF = Ventricular fibrillation; VSD = Ventricular septum defect

Patients

Twenty-two patients were included in this interim report proving the principle, 11 with an overt PS accessory pathway, 6 with an overt LL accessory pathway and 5 with a concealed accessory pathway. The mean age of the patients (11 women) was 41 ± 19 years, range 18-74. They had no structural heart disease, apart from patient WPW02, who had impaired left ventricular function and aortic regurgitation. Baseline characteristics are presented in Table 3.

Ten healthy individuals, in whom VCGs were recorded twice with a one-week interval, served as an external control group, see Study I.

Protocol

Before the ablation procedure, a baseline 12-lead ECG and a VCG were recorded. The RF ablation was performed according to routine. Follow-up recordings were scheduled for 3 and 6 hours post ablation, the day after ablation and then twice a week for 3 weeks and weekly up to 5 weeks, followed by one final visit at least 3 months post ablation. At each follow-up, an ECG and a VCG were recorded.

Analyses

The ECGs were analyzed qualitatively to determine the appearance of T-wave inversions.

The VCGs were analyzed quantitatively to de-

Table 3. Baseline characteristics of 22 patients who underwent a successful radiofrequency ablation of an accessory pathway (AP).

Patient no.	Gender / Age	AP location ECG / ablation site	Drugs prior to ablation	Drugs after ablation
WPW01	M / 23	PS / MCV	None	ASA
WPW02	F / 74	PS / CS os	ACEI, Sotalol	ACEI, ASA, BB
WPW03	M / 41	C / LL	None	ASA
WPW04	M / 38	LL / LL	None	ASA
WPW05	F / 50	LL / LL	Sotalol	ASA, BB
WPW06	M / 18	C / LPS	None	ASA
WPW07	F / 25	LL / AL	BB	ASA
WPW08	F / 64	LL / PL	Beta-stimulator	ASA, beta-stimulator
WPW09	M / 48	PS / CS os	None	ASA
WPW10	M / 22	PS / RPS + LPS	None	ASA
WPW11	M / 62	C / LL	Sotalol, BB	ASA
WPW12	M / 18	C / LL	None	ASA
WPW14	F / 60	PS / RPS	TCA	TCA, ASA, BB (from week 8)
WPW15	F / 20	PS / CS os	OC	ASA, OC
WPW16	F / 31	LL / LL	OC	ASA, OC
WPW19	F / 73	C / LAL	ASA, BB, thyroxin, diuretics	BB, thyroxin, warfarin
WPW20	M / 30	PS / PS + CS os	BB	ASA
WPW21	M / 60	PS / PS + CS os	BB	ASA, BB (week 1), diuretics
WPW103	F / 55	LL / LL	BB, thyroxin	ASA, thyroxin
WPW105	F / 23	PS / RPS	None	ASA
WPW107	M / 27	PS / posterior-PS	None	ASA
WPW108	F / 35	PS / RPS	None	ASA

ACEI = angiotensin converting enzyme inhibitor; AL = anterolateral; ASA= acetylsalicylic acid; BB = beta blocker; C = concealed; CS os = ostium of coronary sinus; LAL = left anterolateral; LL = left lateral; LPS = left posteroseptal; MCV = middle cardiac vein; OC = oral contraceptives; PL = posterolateral; PS = posteroseptal; RPS = right posteroseptal; TCA = tricyclic antidepressants

termine the maximum T-vector amplitude, azimuth and elevation. The VCG parameters from the first day after ablation were compared with the values 1-2 weeks later for each of the 3 groups (PS, LL and concealed accessory pathways). Each parameter was also compared between groups and with the external controls.

VCG analysis (Studies I, II and V)

The VCG recordings were analyzed quantitatively in 3 dimensions. For each recording, the maximum T vector in space was defined and its amplitude and location were calculated. The vector angles were expressed as azimuth and elevation. The VCG was also analyzed in terms of the T-vector loop morphology (Study II), characterized by the three parameters, Tavplan, Tegenv and Tarea, see VCG in Introduction and Figures 9-12.

ECG analysis (Studies II and III)

All ECGs were recorded at a paper speed of 50 mm/s and after a 5-minute stabilization period to allow the rate adaptation of the QT interval [45, 46]. Approximately 10 cardiac cycles of extremity and chest leads were recorded in immediate sequence.

The RR, QRS, QT, QTc, JT and JTc intervals were assessed, as well as QT, QTc, JT and JTc dispersions. Two observers defined the start and end of the QRS complex and the T-wave end. Measurements were then performed by only one of the observers in order to avoid inter-observer variability. Both activities were performed in a blinded fashion, i.e. patient identity and the date of the recording were unknown. The RR, QRS and QT intervals were measured with a digitizing table (Calcomp 2000, Digitizer Products Division, Anaheim, CA, USA), working in point mode (10 lines/mm, accuracy ±0.635 mm). For each lead, an average value for the parameter was calculated from three measured cycles.

In recordings obtained during ventricular pacing, the stimulation artifact defined the onset of QRS. The end of the T wave was defined as the point at which the down-sloping limb of the T wave returned to the iso-electric baseline. If U waves were clearly separated from T waves, the QT interval was measured to the nadir of the curve between the T and the U wave. In the event of partially merging T and U waves, the end of the T wave was defined as the point at which a tangent to the steepest down-sloping limb crossed the iso-electric line [47]. In leads where the T wave could not be identified, those particular leads were excluded from further analysis. The JT interval was calculated in each lead as the difference between the QT and QRS interval. The QRS, QT and JT intervals were presented as a mean value for all measurable leads. The dispersion of the QRS, QT and JT intervals was defined as the difference between the maximum and minimum value of all measurable leads in each ECG. QTc and JTc were calculated according to Bazett, $QT_c = QT \times RR^{-½}$ (RR in seconds, but without unit).

Statistical analysis

Descriptive data are presented as mean ± standard deviation (SD) and range.

Linear regression was used in Study I to analyze the relation between the paced QRS-vector angle and the T-vector angle during *cardiac memory*, as well as the percentage of remaining memory and percentage of paced beats at the last visit. It was also used in Study V for comparisons between maximum T-vector angles post ablation and the preexcited maximum QRS-vector angles prior to ablation.

A one-way repeated measures ANOVA was used in Studies II and III for comparisons of ECG and VCG parameters.

The t-test for dependent samples was used in Study II to compare the ECG parameters during ventricular pacing at baseline and after the development of *cardiac memory*, as well as to compare repolarization time (assessed as JTc) during pacing versus normal conduction both at baseline and at established *cardiac memory*. It was also used in Study V to compare VCG parameters post ablation and after 1-2 weeks, while the t-test for independent samples was used for comparisons between groups**.**

The t-test for dependent samples or Wilcoxon's matched pairs test was used in Study III for comparisons of ECG parameters.

In Study IV, categorical data were compared by contingency tables or cross-tabulation and they

were statistically evaluated using the Chi-square test, Fisher's exact test or the Wilcoxon-Mann-Whitney test. The 95% confidence interval was calculated and presented when appropriate.
A p-value of <0.05 was considered statistically significant.
For details, see Paper I-V.

Results

Time-dependent variations (Studies I, II and V)

The time-dependent variations in repeated VCG recordings were assessed by analyzing the azimuth and elevation of the maximum QRS vector during normal conduction (AAI pacing) in the LT patients at each follow-up visit. The assumption was that the QRS vector would only be minimally affected by periods of ventricular pacing. The mean values for the variations in the QRS vectors compared with baseline were 10 ± 4 º for *azimuth* and 5 ± 2 º for *elevation.*

The time-dependent variations in the maximum T-vector azimuth and elevation were assessed in a group of 10 healthy individuals, in whom VCG was recorded twice with a one-week interval. The mean value for maximum *T-vector azimuth* was 37 ± 11 º (range 7-54 º) and 62 ± 11 º (range 37-76 º) for *T-vector elevation*. The *variations* between the two recordings were 7 ± 5 º for azimuth and 4 ± 3 º for elevation.

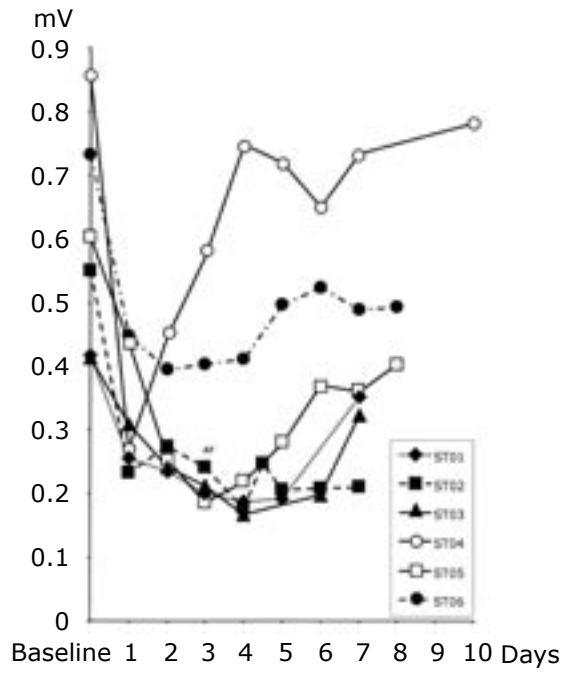

Figure 15. Amplitude of the maximum T vector for the 6 short-term (ST) patients. Each line represents one patient. Patient ST02 developed atrial fibrillation (AF) on day 3. Patient ST06 showed fusion beats on most of the follow-up ECGs and was therefore not fully paced.
Baseline = before pacemaker implantation

Cardiac memory development (Studies I, II and III)

Repolarization assessed during normal conduction

Repolarization changes during normal conduction (temporary AAI pacing), after the initiation of right ventricular endocardial pacing, were analyzed daily in the ST patients (n=6) and weekly in the LT patients (n=14). The earliest signs were observed in the VCG parameters maximum T-vector amplitude and Tarea (not shown). These two parameters displayed very similar behavior with a significant decrease within 24 hours, followed by a significant increase towards baseline values within 1 week; Figures 15 and 16a.

One day later on average (day 1-3 after pacemaker implantation), T-wave inversions were seen in the ECG leads with negative QRS complexes during pacing. Day 1 recordings were also available for 9 of the LT patients and 6 of them (67%) showed new T-wave inversions. At the one-week follow-up, all 14 LT patients showed T-wave inversions on ECG, which remained during the 5- to 8-week follow-up period; Table 4.

After two more days on average (day 2-7 after pacemaker implantation), changes in maximum T-vector azimuth and/or elevation were observed; Figure 17.

At the one-week follow-up, all 14 LT patients showed significant changes in either *azimuth* or *elevation* or *both*. These angles remained virtually unchanged during the follow-up period; Figure 16bc. An average value for the angles from week 1 and throughout the rest of the 5- to 8-week follow-up period was calculated for each individual. In 13 of the14 LT patients,

a. Amplitude

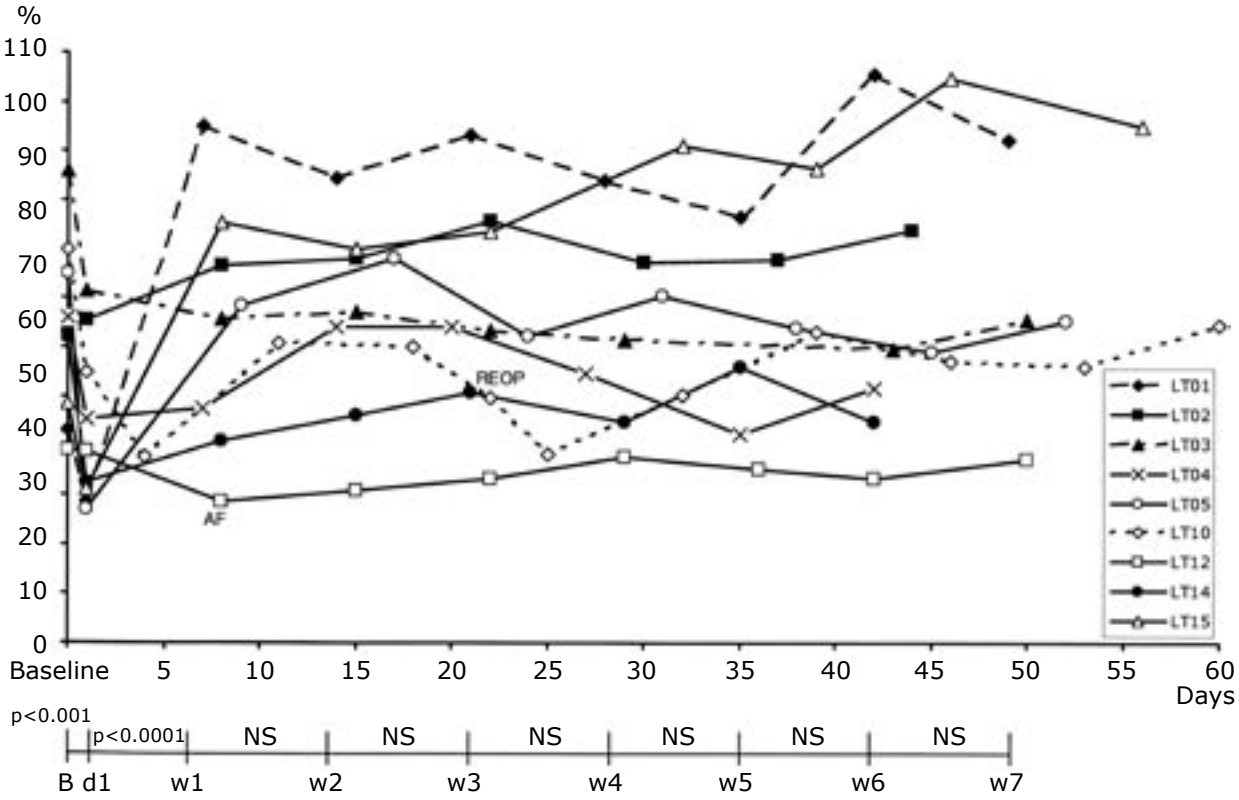

b. Azimuth

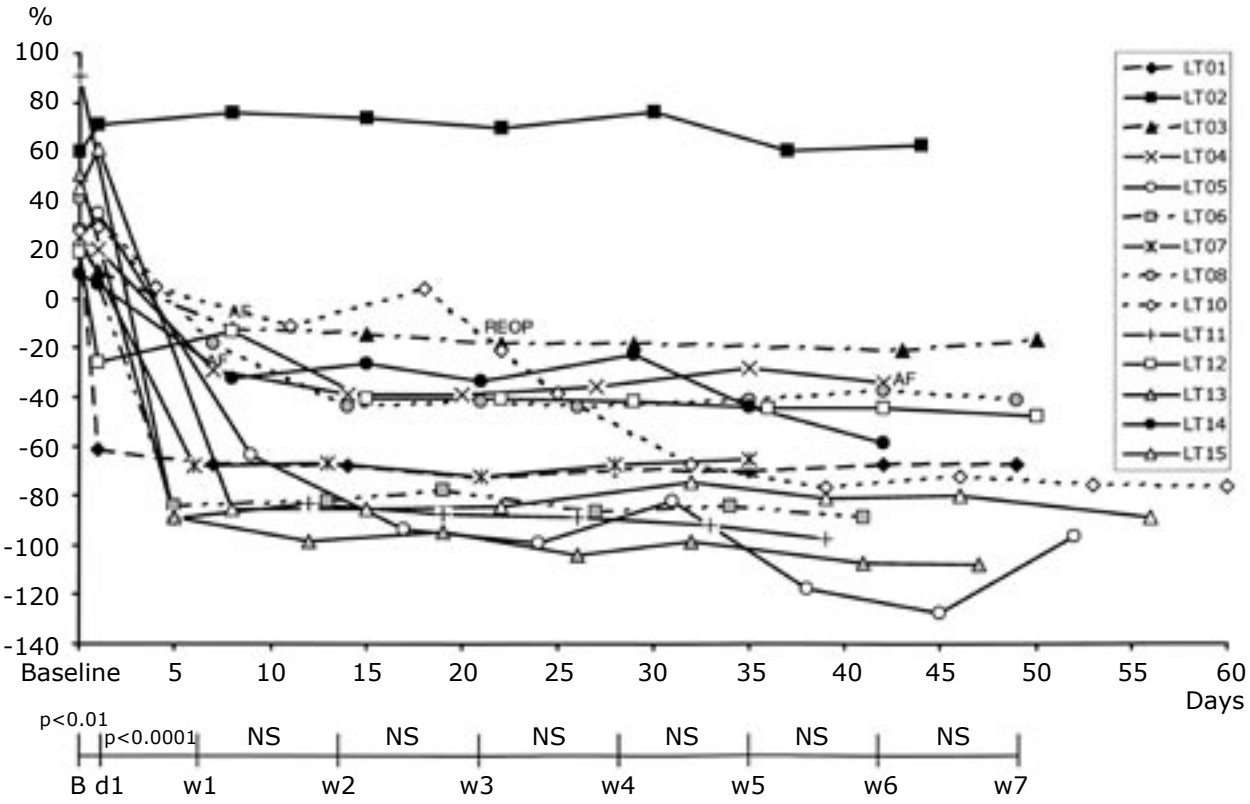

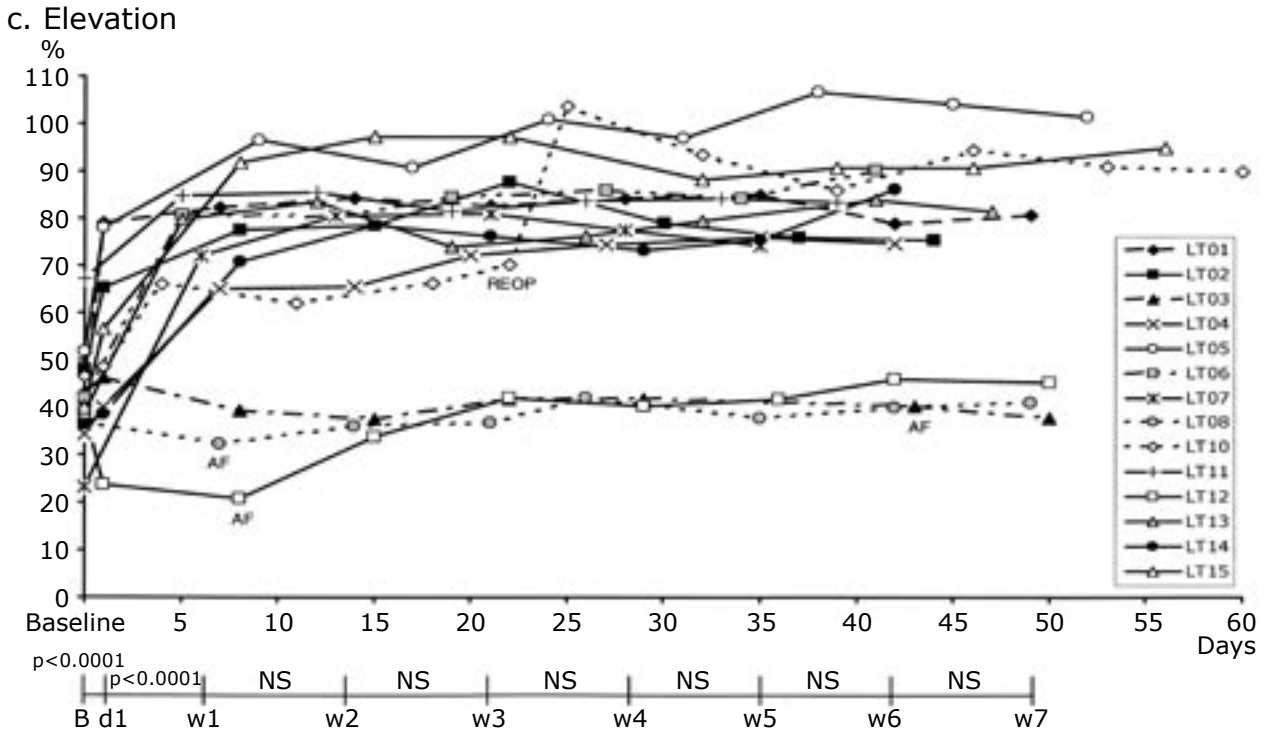

Figure 16. Amplitude (a), azimuth (b) and elevation (c) for the maximum T vector of the 14 long-term (LT) patients during follow-up. Each line represents one patient.

In each patient, the mean value during steady state (w1-8) was calculated for each of the three parameters. The highest mean value in any of the 14 patients was chosen as the reference and the single values for each patient were then expressed as a percentage of the absolute value of this reference. Patient LT10 was re-operated on (REOP) due to dislocation of the ventricular lead after 3 weeks, while patients LT12 and LT08 had atrial fibrillation (AF) at the follow-up visits at 1, and 1 and 6 weeks respectively.

For reasons of clarity, patients in whom recordings from day 1 were not available are excluded in the amplitude graph (LT06, LT07, LT08, LT11, LT13). There was a significant *decrease* in T-vector amplitude from baseline to day 1 ($p<0.001$) and an *increase* from day 1 to week 1 ($p<0.0001$). There was no significant change from baseline to week 1 (a). There was a significant *decrease* in T azimuth from baseline to day 1 ($p<0.01$), from baseline to week 1 ($p<0.0001$) and from day 1 to week 1 ($p<0.0001$) (b). There was a significant *increase* in T elevation from baseline to day 1 ($p<0.0001$), from baseline to week 1 ($p<0.0001$) and from day 1 to week 1 ($p<0.0001$) (c). After week 1, there were no significant changes from one week to the next for any of the parameters.
B = Baseline = before pacemaker implantation
d1 = day 1
w1, w2 etc = week 1, week 2 etc.

Table 4. Fourteen patients were endocardially paced in the right ventricle with a short AV delay for 5-8 weeks (phase 1), followed by 4-5 weeks of pacing with a long AV delay (phase 2). Columns 2 and 3 show the presence of *cardiac memory* (T-wave inversions, TWI) on ECG after 1 day and 1 week respectively. Column 4 shows the presence of *cardiac memory* after 4-5 weeks of pacing with a longer AV delay, while column 5 shows the extent of ventricular pacing during phase 2.

Patient	TWI Day 1	TWI Week 1	TWI Last visit	% pacing Last visit
LT01	Yes	Yes	Yes	100 %
LT02	Yes	Yes	Yes	77 %
LT03	No	Yes	Yes	78 %
LT04	Yes	Yes	No	51 %
LT05	Yes	Yes	No	0 %
LT06	---	Yes	No	3 %
LT07	---	Yes	No	44 %
LT08	---	Yes	Yes	79 %
LT10	No	Yes	Yes	100 %
LT11	---	Yes	Yes	63 %
LT12	Yes	Yes	Yes	38 %
LT13	---	Yes	Yes	94 %
LT14	No	Yes	Yes	100 %
LT15	Yes	Yes	No	40 %

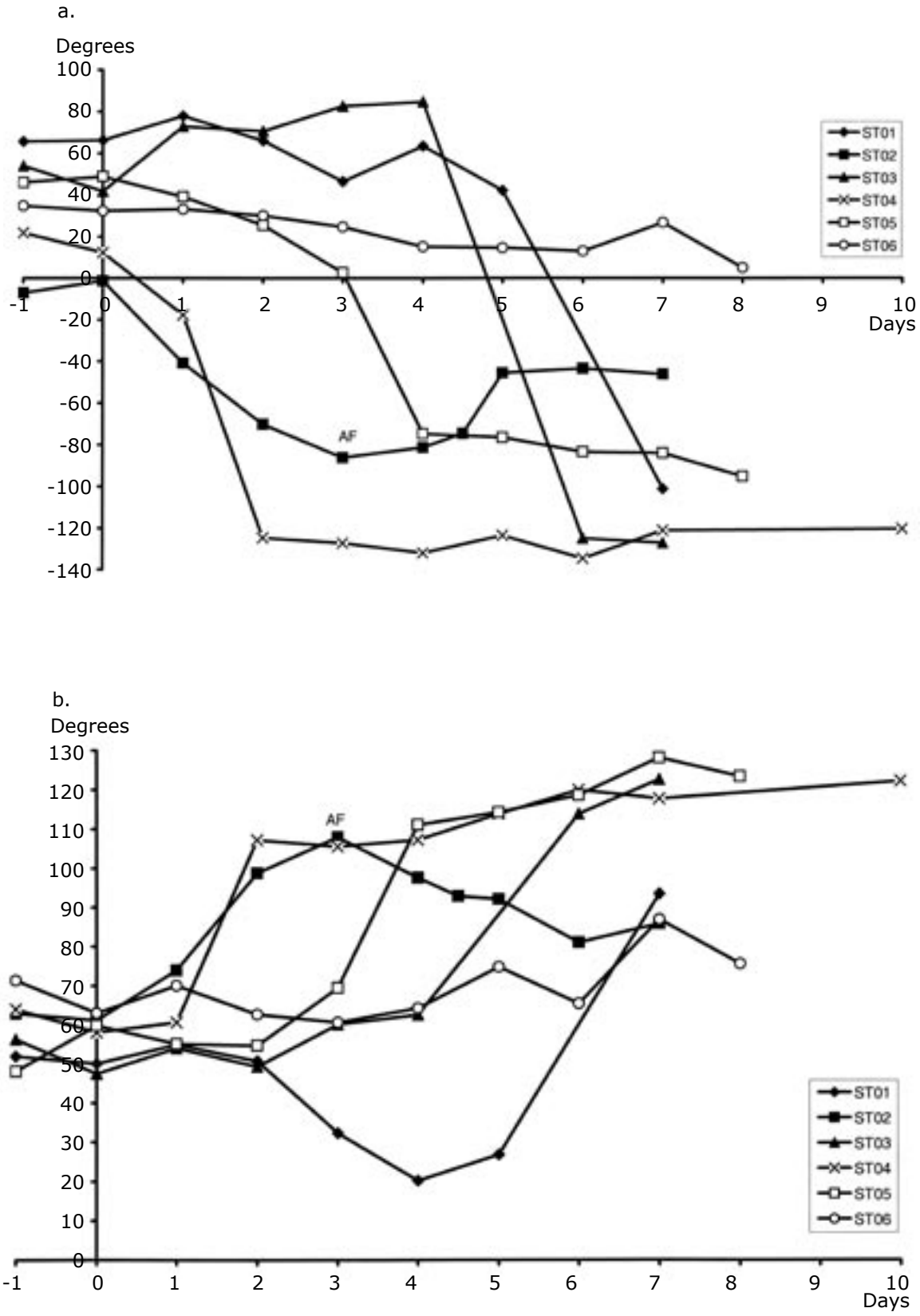

Figure 17. Maximum T-vector azimuth (a) and elevation (b) for the 6 short-term (ST) patients. Each line represents one patient. Patients ST01, ST03, ST04 and ST05 were paced for >90% of the time, except for day 1 (62%) and day 5 (87%) for patient ST01. Patient ST06 showed fusion or pseudo-fusion on most of the ECGs during follow-up, due to enhanced AV conduction. Patient ST02 had atrial fibrillation (AF) on day 3 and DC conversion failed.
Adapted from Study I.

there was a significant change in *T-vector azimuth* (backward rotation) with a mean of –150°, range –286-(-60)°. For 11 patients, there was a significant change in *T-vector elevation* (in the cranial direction) during the same period, with a mean of 63°, range 26-84°. The only patient (LT02) without any significant change in T-vector azimuth showed a significant change in T-vector elevation. All these changes were generally more than 10 times as large as the time-dependent variations over one week in healthy controls; Figure 18.

There was a statistically significant correlation between the angles (azimuth and elevation) of the *paced* maximum QRS vector and the angles of the maximum T vector during normal conduction after the development of *cardiac memory* (azimuth: $r = 0.75$, $r^2 = 0.57$, $p<0.05$, n=8; elevation: $r = 0.80$, $r^2 = 0.64$, $p<0.01$). This is in line with the definition of *cardiac memory* based on ECG, where the T-wave vector during *cardiac memory* "tracks" (or remembers) the vector of the paced QRS complex; Figure 19.

The *frontal plane* T-vector angle (used in the dog model) did not change in 4 of 14 patients (29%). As a result, in human subjects, the analysis of the maximum T-vector angle in space, assessed as azimuth and elevation *in combination*, was a more sensitive method for detecting *cardiac memory* development than was the frontal plane vector *alone*; Figure 20.

On the second to third postoperative day, Tegenv displayed a significant decrease, consistent with a more circular loop. On a long-term basis (> 1 week), however, Tegenv did not display any clear pattern. Tavplan displayed considerable inter- and intra-individual variations during the first few days, but it increased significantly to the one-week follow-up and then remained stable.

After 35-43 days of ventricular pacing, the rate-adjusted QT interval, QTc, was significantly prolonged by 25 ms or 6% at normal conduction compared with baseline values (QTc 429 ± 33 vs. 454 ± 46 ms, $p< 0.05$). There were no significant changes in QT or JT dispersion.

In all patients with HOCM (n=15), new T-wave inversions were observed after ≥ 3 months of ventricular pacing. In contrast to the control group, the HOCM patients did not show any significant change in repolarization time (QTc) associated with the development of *cardiac memory.*

Repolarization assessed during ventricular pacing

For this post-hoc analysis, ECGs *during* pacing were available both from the day of pacemaker implantation and from the last follow-up after 5-8 weeks of right ventricular pacing in 6 of the LT patients. There was a significant decrease in the mean QTc by 49 ms or 9% and in the mean JTc by 38 ms or 11% *during* ventricular pacing from the first day to the last follow-up (QTc 518 ± 20 vs. 469 ± 26 ms, and JTc 342 ± 28 vs. 304 ±19 ms, $p < 0.01$ for both comparisons). During the first week, however, there seemed to be no significant change as judged from the ST patients (n=5).

When comparing JTc *during* pacing on the day of implantation with the baseline JTc (sinus rhythm before pacemaker implantation), there was no difference. However, after 5-8 weeks of ventricular pacing, JTc *during* ventricular pacing was significantly shorter by 43 ms or 12% than during normal conduction (AAI pacing) at the same basic rate (JTc 304 ±19 vs. 347 ±35 ms, $p< 0.01$). Also in the HOCM patients (n=15), a shortening of the repolarization time (JTc) during pacing was observed. After ≥ 3 months of DDD pacing, the JTc interval *during* DDD pacing was 24 ms or 7% shorter on average than during subsequent sinus rhythm with normal ventricular activation (329 ± 25 ms vs 353 ± 21 ms; $p < 0.05$). When the 30 HOCM patients who had not been studied at baseline were added, the JT interval during DDD pacing was 8% shorter compared with the post-pacing sinus rhythm (316 ± 34 ms vs 343 ± 37 ms) and the JTc interval was 5% shorter (337 ± 22 ms vs 355 ± 25 ms; $p<0.001$ for both).

Presence of cardiac memory after WPW ablation (Studies IV and V)

In the retrospective study of patients with overt PS accessory pathways, *cardiac memory* was observed in 123 of 125 (98%) of the patients within one day after successful RF ablation. Concordance between post-ablation T-wave polarity and *QRS polarity* prior to ablation in leads II, aVF and III respectively was found in

a. Azimuth

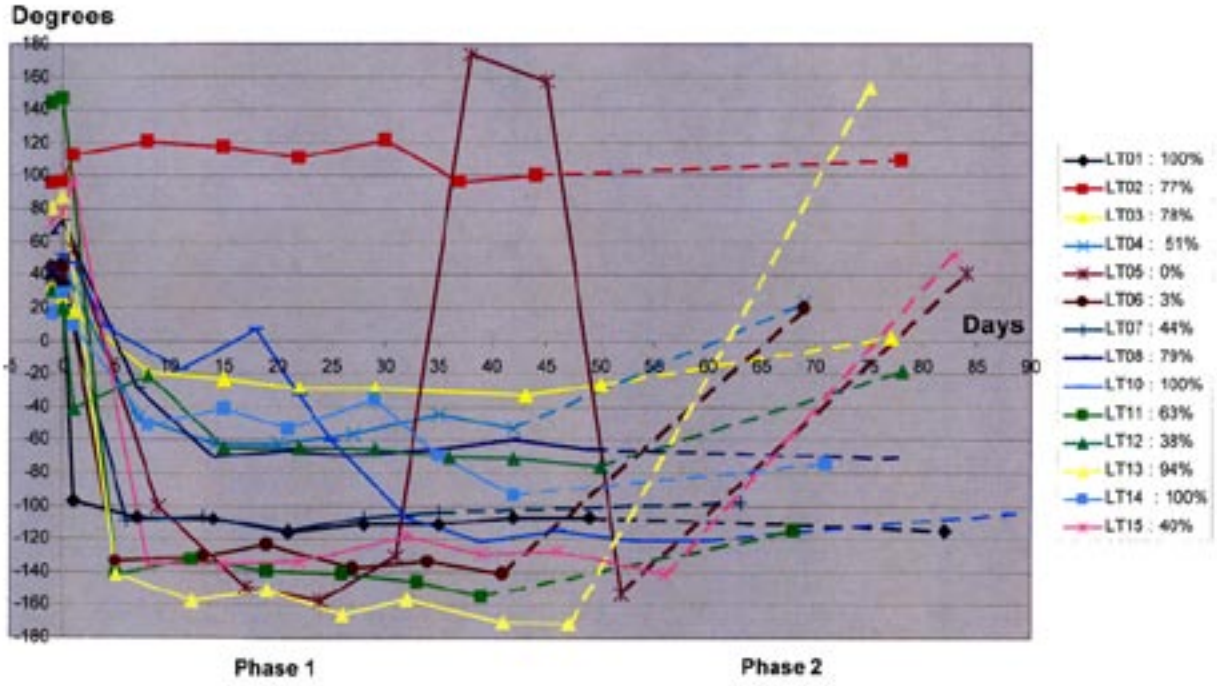

b. Elevation

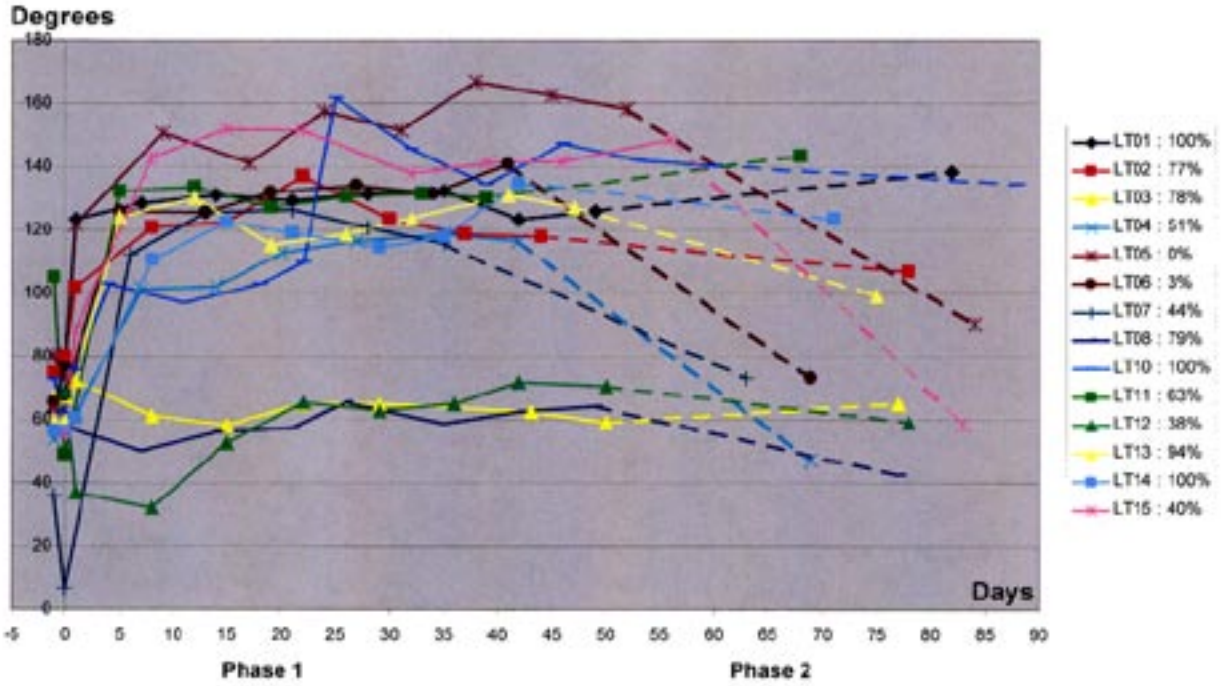

Figure 18. T-vector azimuth (a) and elevation (b) for the 14 long-term (LT) patients. Each solid line represents one patient during the 5- to 8-week follow-up period, while the broken line is followed by the value from the last visit after the pacemaker had been individually programmed. The amount of pacing during the weeks before the last visit for each patient is shown to the right. All patients apart from LT02 showed a significant backward rotation of the T vector (azimuth, 18a), and all but 3 (LT03, LT08 and LT12) displayed a significant cranial rotation (elevation, 18b). Because azimuth is defined as ± 180º (Figure 9), there is a "jump" in the line representing patient LT05 (week 5-6), when the angle exceeds -180º and by definition becomes positive. Similarly, during the period before the last visit, patient LT13 was paced for 94% of the cardiac cycles and actually retained memory (elevation, 18b), with an azimuth exceeding -180º, which therefore became positive (18a). Patient LT10 had a stepwise increase related to ventricular lead repositioning during the third week.

69%, 82% and 89%, while the corresponding figures for *delta wave polarity* were 57%, 75% and 88%, with overlapping 95% confidence intervals for each lead.

In this special case of ablation of an overt PS accessory pathway, the resolution of *cardiac memory* always started with the normalization of lead II, followed by lead aVF, while the last to normalize was lead III. We therefore tentatively used the number of leads with T-wave inversions as an estimate of the degree of *cardiac memory*. Assessed in this way, there was significantly "stronger" memory in patients aged > 50 years compared with patients aged < 20 years one day after the ablation procedure ($p < 0.01$); Figure 21. There was, however, no correlation between the degree of preexcitation and the degree of *cardiac memory* after ablation.

In the prospective study, all patients ablated due to an overt PS accessory pathway (n=11) showed T-wave inversions in 2 or 3 of the inferior leads (II, aVF, III) after ablation. There were no abnormal T-wave inversions following ablation of either LL (n=6) or concealed (n=5) accessory pathways.

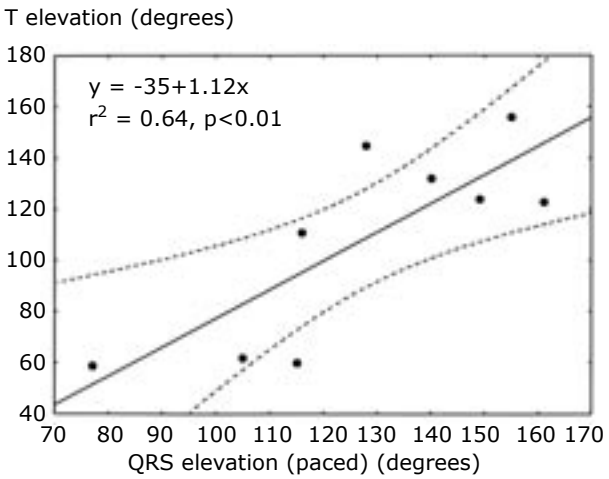

Figure 19. There was a statistically significant correlation between the vector angles azimuth (not shown) and elevation of the paced QRS and the angle of the T vector during *cardiac memory* in 9 cases with technically satisfactory recordings during ventricular pacing. In 5 patients, recordings could not be made because of interaction between the pacing artifact at QRS onset and the equipment.

Reprinted from Study I with permission from the publisher.

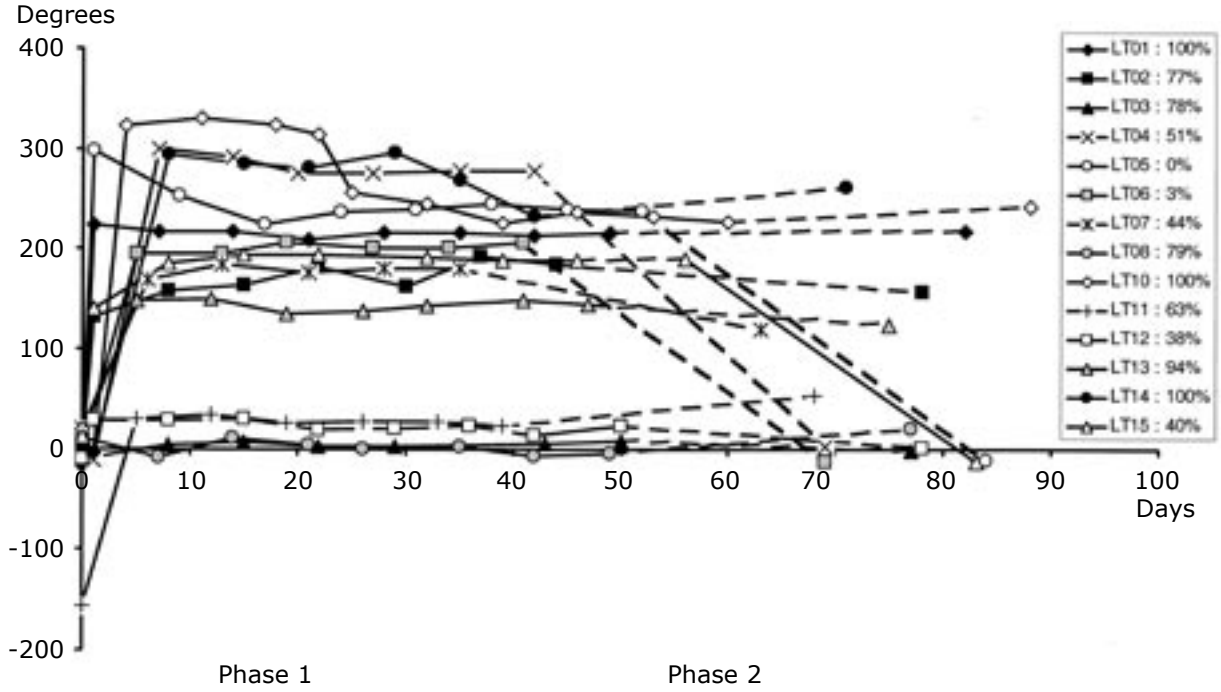

Figure 20. Changes in the frontal plane T vector for the 14 long-term (LT) patients. In four patients (28%), there was no change. Each solid line represents one patient during the 5- to 8-week follow-up period, while the broken line is followed by the value from the last visit after the pacemaker had been individually programmed. The amount of pacing during the weeks before the last visit for each patient is shown to the right.

VCG analysis revealed a moderate to strong correlation between the maximum T vector post ablation and the preexcited maximum QRS vector (elevation: $r = 0.83$, $r^2 = 0.68$, $p < 0.0001$, azimuth: $r = 0.49$, $r^2 = 0.24$, $p < 0.05$). This is in line with the ECG-based definition of *cardiac memory*.

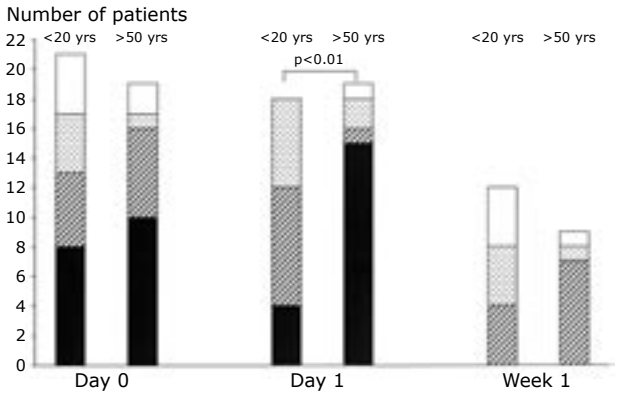

Figure 21. Number of the youngest (< 20 years) and oldest (> 50 years) patients with memory signs in leads II, aVF and III, immediately after ablation, the next day and after 1 week (6-8 days). Patients with memory signs in all inferior leads ■, in leads aVF and III ▨, in lead III ▦ and without memory signs □.
Adapted from Study IV.

VCG analysis of the maximum T vector within one day after ablation revealed a significantly higher *elevation* value in the PS group compared with each of the other 3 groups (LL, concealed and controls). The LL group, on the other hand, had a significantly higher T-vector *azimuth* value compared with the concealed accessory pathway group and healthy controls.
There was no significant change in any parameter in the group which had a concealed accessory pathway ablation, or in the control group; Table 5.

Cardiac memory dissipation (Studies I, IV and V)

Dissipation of cardiac memory after the cessation of ventricular pacing

Since the AV delay was optimized for each of the LT patients during the weeks before the last visit, some patients continued to be paced in the ventricle 100 % of the time, while some were not paced at all and others were paced to a variable extent; Figure 18. This variation in the percentage of paced cardiac cycles provided an opportunity to analyze the relationship between the amount of pacing and the amount of retained memory.

Table 5. Elevation and azimuth of the maximum T vector within one day after the successful radiofrequency (RF) ablation of an accessory pathway (AP) and after 1-2 weeks. Healthy controls were not RF ablated. Mean ± SD (standard deviation). AP = accessory pathway; PS = posteroseptal; LL = left lateral

		PS AP (n=11)	**LL AP** (n=6)	**Concealed AP** (n=5)	**Healthy controls** (n=10)
T elevation					
Day	1	101 ± 14° ** ###	63 ± 14°	55 ± 9°	62 ± 12°
Week	1-2	75 ± 15° #	57 ± 12° (n=5)	57 ± 6°	62 ± 12°
T azimuth					
Day	1	51 ± 23°	69 ± 10° * ###	39 ± 6°	36 ± 14°
Week	1-2	43 ± 28°	44 ± 15° (n=5)	41 ± 9°	39 ± 8°

Within-group comparisons (columns):
* $p < 0.05$ for comparisons between T-vector *azimuth* day 1 and week 1-2
** $p < 0.01$ for comparisons between T-vector *elevation* day 1 and week 1-2

Between-group comparisons (rows):
\# $p < 0.05$ for comparisons between PS and each of the other groups respectively
$p < 0.001$ for comparisons between PS and each of the other groups respectivly and for comparisons between LL and the concealed and control group respectively

ECG: The ECG from the last visit showed T-wave inversions in 9 of the patients, 8 of whom were paced in the ventricle for > 60 % of the time during the last 4-5 weeks. Six patients were paced for < 60% of the time and 5 of them showed no T-wave inversions; Table 4.

VCG: In each of the 13 patients with T-vector azimuth changes, the remaining *cardiac memory* was calculated as the T-vector azimuth change at the last visit *divided* by the mean T-vector azimuth change from week 1 throughout the 5- to 8-week follow-up period; Figure 22a. The same calculations were performed for the 11 patients with changes in T-vector elevation; Figure 22b. There seemed to be a linear relation between the percentage of remaining *cardiac memory* and the percentage of ventricular paced cardiac cycles. When ventricular pacing was completely disrupted, cardiac memory disappeared within 4 weeks.

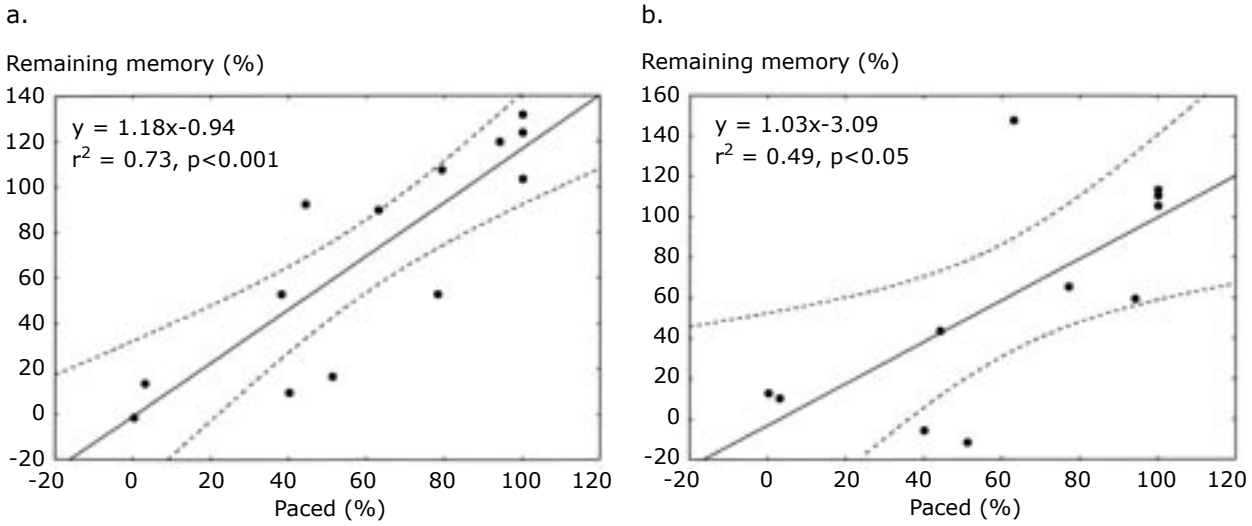

Figure 22. Remaining *cardiac memory* (T-vector changes) at the last visit (as a percentage of the mean value for *cardiac memory* during follow-up) related to percentage of ventricular pacing, 13 patients with T-vector azimuth changes (a) and 11 with T-vector elevation changes (b).
Reprinted from Study I with permission from the publisher.

Table 6. Number of patients with ECG signs of *cardiac memory* in inferior leads after WPW ablation (95% confidence interval). From top to bottom increasing degree of memory.

Inferior leads with T-wave changes	**Day 0** n = 122	**Day 1** n= 110	**Week 1** (day 6-8) n = 49	**Month 1-2** (day 30-60) n = 17	**Month 2-3** (day 61-91) n = 13	**Month 3-6** (day 92-182) n = 27	**Month >6** (day >182) n = 20
None (95% CI)	15 (12%) (6-18%)	3 (3%) (0.6-7.8%)	9 (18%) (8-29%)	5 (29%) (10-56%)	11 (85%) (55-98%)	17 (63%) (42-81%)	12 (60%) (36-81%)
III (95% CI)	14 (11%) (6-17%)	23 (21%) (13-29%)	18 (37%) (23-50%)	8 (47%) (23-72%)	2 (15%) (1.9-45%)	8 (30%) (14-50%)	6 (30%) (12-54%)
aVF, III (95% CI)	33 (27%) (19-35%)	32 (29%) (21-38%)	20 (41%) (27-55%)	3 (18%) (3.8-43%)	0	2 (7%) (0.9-24%)	2 (10%) (1.2-32%)
II, aVF, III (95% CI)	60 (49%) (40-58%)	52 (47%) (38-57%)	2 (4.1%) (0.5-14%)	1 (5.9%) (0.2-29%)	0	0	0

CI = Confidence Interval
Reprinted from Study IV with permission from the publisher.

Dissipation of cardiac memory after WPW ablation

As mentioned above, *cardiac memory* (T-wave inversions) was observed in 123 of 125 (98%) of the patients within one day after successful RF ablation. One week after ablation, an ECG was available in 49 patients and *cardiac memory* was present in 40 (82%), while after 1-2 months it was present in 12 of 17 (71%). More than 6 months after ablation, 12 of 20 ECGs (60%) had no T-wave changes at all, 6 had changes in one inferior lead and 2 in two inferior leads; Table 6; Figure 23.

In the prospective study, the maximum T-vector elevation was significantly higher both on day 1 and after 1-2 weeks in the PS accessory pathway group compared with each of the other 3 groups (LL, concealed and controls). Despite this, T elevation decreased significantly from the first day to the follow-up visit 1-2 weeks later (101 ± 14° vs. 75 ± 15°, $p < 0.005$).

The high maximum T-vector azimuth value in the LL accessory pathway group decreased significantly from day 1 to week 1-2 (70 ± 11° vs. 44 ± 15°, $p < 0.05$, $n = 5$); Table 5.

The dissipation of *cardiac memory* over time for the different patient groups is shown in Figure 24. In 14 of 17 (82%) patients, *cardiac memory* had disappeared within 3-4 weeks.

Cardiac memory – good, bad or neutral (Studies II and III)

Based on the observed decrease in Tegenv and increase in Tavplan, both of which are associated with increased repolarization heterogeneity, and the prolongation of QTc, the development of *cardiac memory* may be accompanied by a potentially deleterious effect on ventricular repolarization when abruptly switching from ventricular pacing to normal conduction. In contrast, there was a significant decrease in repolarization time *during* extended ventricular pacing, both in patients with structurally normal or close to normal hearts and in patients with HOCM.

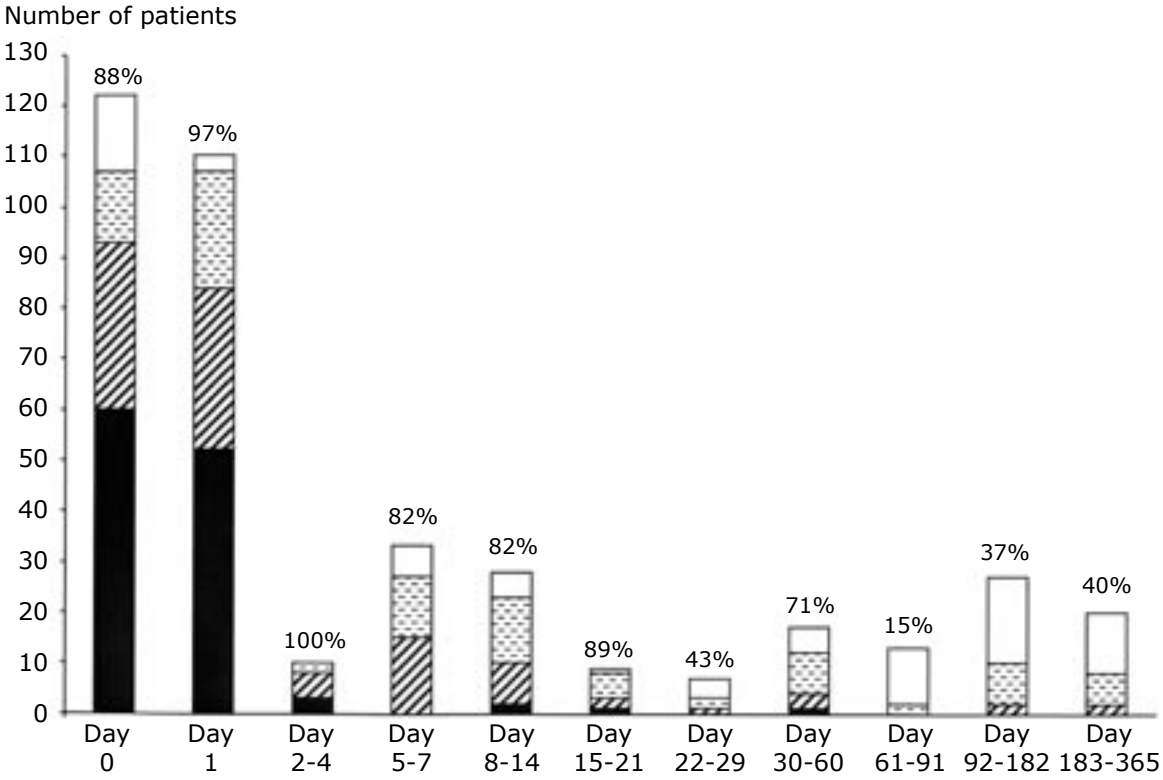

Figure 23. Number of patients with memory signs in leads II, aVF and III, immediately after ablation and up to one year post ablation. Patients with memory signs in all inferior leads ■, in leads aVF and III ▨, in lead III ▦ and without memory signs □. The percentage of patients with T-wave inversion in at least one lead is shown for each interval.
Adapted from Study IV.

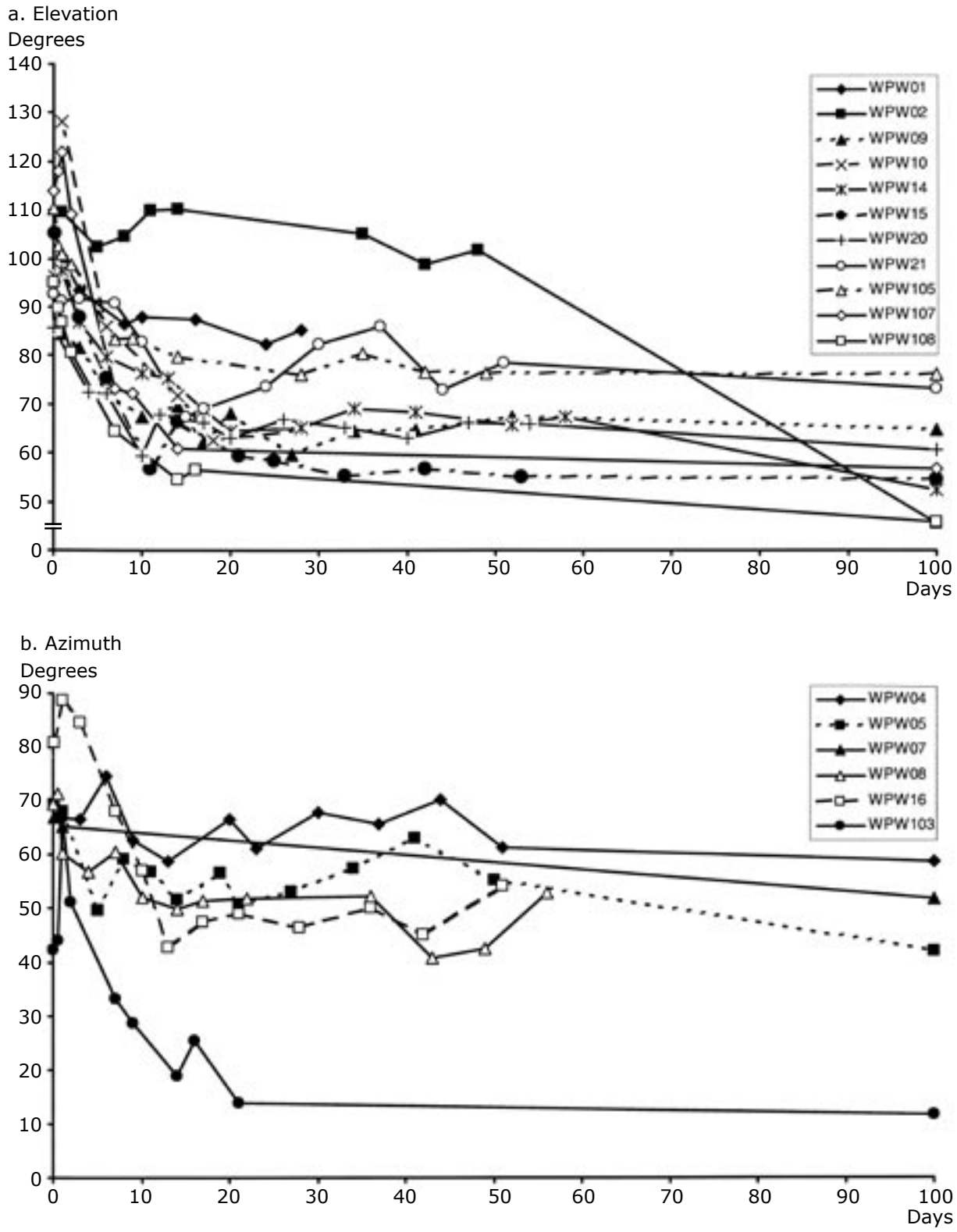

Figure 24. Dissipation of *cardiac memory* after the radiofrequency ablation of overt accessory pathways. Each line represents one patient.

a) *Cardiac memory* in patients ablated due to an overt posteroseptal accessory pathway was reflected by high T-vector elevation values.

b) *Cardiac memory* in patients ablated due to an overt left lateral accessory pathway was reflected by high T-vector azimuth values.

Summary of results

- The T vector during *cardiac memory* (normal conduction) correlated with the QRS vector during the previously altered activation sequence. This was true for both the pacing and the WPW (preexcitation) model and was consistent with the original ECG-based definition of *cardiac memory*.
- The VCG parameters maximum T-vector amplitude and Tarea detected *cardiac memory* related repolarization changes in the human pacing model within 24 hours. This was before T-wave inversions could be recognized on the conventional 12-lead ECG.
- *Cardiac memory* development reached steady state within one week after the onset of right ventricular endocardial pacing at physiologic rates and was faster and more homogeneous in time than expected.
- *Cardiac memory* development might result in different repolarization responses depending upon baseline structure and electrophysiology. HOCM patients displayed similar morphological T-wave changes, but the repolarization time response was different compared with controls.
- In the pacing model, after approximately 4 weeks of pacing with a longer AV delay, *cardiac memory* was preserved in proportion to the percentage of ventricular pacing. This relation seemed to be linear.
- If ventricular pacing was completely discontinued, *cardiac memory* disappeared within 4 weeks.
- Changes in the QT interval and T-vector loop morphology imply that *cardiac memory* development might be accompanied by unfavorable repolarization changes.
- *Cardiac memory* was observed in 98% of the patients within one day after the successful RF ablation of an overt PS accessory pathway.
- *Cardiac memory* was present after the successful RF ablation of overt accessory pathways, independent of the accessory pathway location. Repolarization changes after the ablation of PS accessory pathways were mainly expressed in the vertical direction and, after the ablation of LL accessory pathways, mainly in the transverse plane.
- *Cardiac memory* appearing after the successful RF ablation of an overt PS accessory pathway disappeared in the majority of available ECGs within 3 months but persisted for longer than 6 months in some patients.

General Discussion

In recent decades, *cardiac memory* has evolved from being an electrocardiographic curiosity to a concept of potential clinical importance, not only as a diagnostic confounder regarding myocardial ischemia. This thesis focuses on the occurrence, development and dissipation of *cardiac memory* in two human models, ventricular pacing and ablation of the WPW syndrome. In order to expand our knowledge of repolarization changes associated with *cardiac memory*, we used VCG analyzed in 3 dimensions, including the T-loop morphology analysis, as well as conventional ECG. VCG facilitates the quantification of T-vector changes, which was shown as part of the methodological development. In addition, potential positive and negative effects of *cardiac memory* on repolarization in the human heart were addressed. In parallel with our studies, other groups have focused on the mechanisms of *cardiac memory*, mainly by pursuing studies in the canine model of ventricular pacing.

Definition of cardiac memory

The definition of *cardiac memory*, which has primarily been established from ECG studies, is as follows:

T-wave inversions on ECG during normal ventricular activation following a period of previous abnormal ventricular activation, where the T- wave vector tracks the previously altered QRS vector. During continuous normal ventricular activation, the T wave will slowly normalize.

Our studies using VCG confirmed that the T vector tracks the previously altered QRS vector, both in the human pacing model and after the ablation of the WPW syndrome, results that corroborate the definition of *cardiac memory.*

Cardiac memory and ventricular pacing

In humans, *cardiac memory* developed and reached steady state within one week after the onset of endocardial pacing in the right ventricular apex at physiologic rates. This was the main finding in Study I, where *cardiac memory* was evaluated by means of qualitative ECG analysis and analysis of the T-vector angles of the VCG. Further analysis (Study II) showed that repolarization changes in the form of reduced maximum T-vector amplitude and decreased Tarea could already be detected within the first 24 hours after the onset of right ventricular endocardial pacing.

Other studies of *cardiac memory* related to ventricular pacing in humans have mainly used the ECG [3, 14, 17], whereas VCG has been applied in studies of dogs [18]. Chatterjee et al. studied 31 patients, 30 who were paced endocardially and one epicardially, and found massive T-wave inversions post pacing in all patients, apart from two who had LBBB. The duration of ventricular pacing varied from 10 minutes to 4 years. Five patients were followed for up to 2 weeks and they showed increasing T-wave inversions. The authors did not specifically study the temporal characteristics of *cardiac memory* dissipation but noted that 10 minutes of ventricular pacing led to T-wave changes that persisted for 15 minutes, while 2 years of pacing caused changes that were still present after 18 months. It is not clear whether the latter patients were temporarily paced during this period [3].

Rosenbaum et al., who introduced the concept of *cardiac memory*, studied 85 patients with intermittent LBBB and found T-wave changes during normal conduction which "remembered" the QRS of the abnormal conducted beats (i.e. had the same vector) verified by both ECG and VCG. They also studied (using ECG) the effect of right ventricular pacing, usually creating a

LBBB pattern, in 5 patients paced for between 25 and 66 hours at rates of 100-120 beats/min, and concluded that the T-wave changes progressed gradually and uniformly, although they did not reach steady state in any of the patients. The return to a normal ECG took 8-38 days (4 patients), although *not* from a steady state level (fully developed *cardiac memory*). In addition to the cumulative effect of *cardiac memory*, they also found that repeated trains of ventricular pacing of 15 minutes' duration, separated by non-pacing intervals allowing for T-wave changes to disappear, induced a greater degree of T-wave changes for each successive train. The heart therefore appeared to "remember" that the activation sequence had been abnormal some time ago, as well as the direction of it [14].

Alessandrini et al. studied *cardiac memory* in 8 patients paced from the ventricle at 70-80 beats/min for 1 hour and 1 week respectively but only observed *cardiac memory* in the one-week group. The question of whether or not steady state was reached after 1 week of pacing was not addressed. The T-wave inversions persisted for the entire observation time of 24 hours [17].

In dogs, Shvilkin et al. applied both ECG and reconstructed VCG in the frontal plane to study *cardiac memory* development and dissipation. The animals were paced epicardially from the left ventricle and at a rate 10-15% faster than the animals' sinus rhythm. While the T-vector amplitude increased and reached steady state after about 10 days, the T-vector angle did not reach steady state until about 3 weeks of ventricular pacing [18]. This is partly different from our results in humans. Firstly, we found an initial *decrease* in maximum T-vector amplitude within 24 hours after the onset of ventricular pacing, followed by an increase towards baseline values within one week. Secondly, changes in the maximum T-vector angle (azimuth and/or elevation) reached steady state within one week after the initiation of ventricular pacing in humans, which is about 3 times faster than in the dog model.

The different results were unexpected, since our hypothesis was that the development of *cardiac memory* in humans would be both *slower,* due to a lower heart rate, and more heterogeneous than in the dog model. Possible explanations for the different results in humans compared with dogs in these studies are:

1. Different species: humans vs. dogs.
2. Different pacing sites: endocardial right ventricular pacing in humans vs. epicardial left ventricular pacing in dogs.
3. Different extent of ventricular pacing:
   > 90% ventricular pacing in humans vs.
   > 75% ventricular pacing in dogs.
4. Different analysis of the VCG:
   3-dimensional analysis in humans vs. only frontal plane analysis of a reconstructed (from ECG) VCG in dogs.

In general, the ECG features were very similar in dogs and humans. It therefore appears to be unlikely that species differences play a major role.

With regard to pacing site, there were two differences; i.e. the left versus the right ventricle and epicardial versus endocardial pacing. As judged from the WPW experience, where there were no major differences in memory expression between left and right accessory pathway sites, it does not seem very likely that the difference in stimulated ventricle plays a major role. When it comes to epicardial versus endocardial pacing, there are some intriguing differences to consider. Epicardial stimulation originates remotely from the specialized Purkinje system compared with endocardial pacing. In addition, the myocardial layers are arranged differently. So, in the canine wedge preparation, epicardial stimulation resulted in a slower transmural conduction velocity and a longer conduction time, as well as a less planar activation wave front, compared with endocardial stimulation [48]. The morphology of the wave front is important for the safety of conduction (source to sink relationship, see page 15). These heterogeneities across the transmural wall are probably due to the reduced expression of gap junctions in the subepicardial layers relative to the deeper myocardial layers [49]. For this reason, the temporal differences are most likely related to the different pacing sites, but this needs to be confirmed. According to preliminary data right ventricular endocardial pacing in the dog

gives similar results as in our human model (MR Rosen, personal communication).
The extent of ventricular pacing (percentage of impulses with altered activation) required to reach a steady state of *cardiac memory* is uncertain. We arbitrarily chose a goal of > 90% ventricular paced cardiac cycles, which was met for the majority of the patients according to the pacemaker log. Shvilkin et al. monitored 4 dogs for 24 hours on random days and found capture > 75% of the time [18]. It is possible that the temporal difference mentioned above is partly explained by the different extent of ventricular pacing, which may also have been < 75% in the dogs for some time.
The different behavior of maximum T-vector amplitude may be explained by the different analyses that were used. When only the frontal plane was analyzed in humans, 4 of 14 (29%) patients did not show any change in the T-vector angle.

The **dissipation** of *cardiac memory* required approximately 7 days in dogs paced for 21-25 days and > 30 days (more than the observation time) in dogs paced for 42-52 days [18].
In our study, *cardiac memory* in humans disappeared within 4 weeks when pacing was disrupted after 5-8 weeks of ventricular pacing. According to the ECG analysis, T-wave changes persisted when the amount of ventricular pacing was > 60% of the time. However, this reflects the amount required to retain already established *cardiac memory*. VCG analysis (T-vector azimuth/elevation) showed that, after approximately 4 weeks of pacing with a longer AV delay, *cardiac memory* was conserved in proportion to the percentage of ventricular pacing, a relation that seemed to be linear. This is a novel finding, which shows similarities with psychological memory studies [16].

When we compared the rate-adjusted QT interval (QTc) during normal conduction before pacemaker implantation with that during normal conduction (temporary AAI pacing) after 5-6 weeks of ventricular pacing, i.e. during *cardiac memory*, we found a significant prolongation of 25 ms or 6 %. Data from previous studies in humans are conflicting. Neither Chatterjee et al. nor Rosenbaum et al. found any consistent changes in QTc [3, 14]. Chatterjee et al. found an increase in 13 patients and a decrease in 15 but the duration of pacing varied tremendously, from 10 minutes to > 4 years [3]. Alessandrini et al., on the other hand, found a non-significant prolongation of QT of 3% at 3 minutes after the cessation of 1 week of ventricular pacing compared with baseline values. Thereafter, QT decreased significantly by 4% to the next day [17], which is in line with our results.
In right ventricular epicardially paced dogs, no consistent change in QTc was observed in the short-term memory model (3 x 20 minutes of pacing) [21]. In the long-term memory model, Plotnikov et al. found an increase in QT interval of approximately 7% during normal conduction after 21 days of epicardial left ventricular pacing compared with baseline values [50], similar to our results. In two other long-term memory studies using the same model, a prolongation of APD of endocardial and epicardial myocytes was found when analyzing myocardial strips, but QT and QTc were unchanged [18, 51].

When the repolarization time *during* ventricular pacing was assessed, the opposite result was obtained. After 5-8 weeks of right ventricular pacing, we found a significant decrease in the mean QTc of 49 ms or 9 % and in the mean JTc of 38 ms or 11 %. This is in line with the results reported by Alessandrini et al., who observed that the QT interval during pacing was significantly longer after 1 hour compared with after 1 week of ventricular pacing in humans [17]. In the long-term dog model, on the other hand, a prolongation of QT during pacing was observed after 21 days of epicardial left ventricular pacing [50].

The changes in QTc associated with the development of *cardiac memory* in humans suggest an adaptive process to the new activation sequence, in accordance with the observations in the Langendorff-perfused rabbit heart [52].

Cardiac memory and HOCM

The right ventricular endocardially paced HOCM patients displayed a similar morphological ECG pattern of *cardiac memory* to that displayed by the control patients with structurally normal or almost normal hearts. This is in line with a previous study by McAreavey et al.,

who examined the relationship between electrical changes and alterations in the left ventricular hemodynamic state in 18 HOCM patients. They examined the amplitudes of the R, S and T wave on ECG and found that the T wave became more negative in inferior and lateral leads in 13/18 patients, which they called "electrotonic modulation" of the T wave [53].

In contrast to the control group, the development of *cardiac memory* was *not* associated with any change in repolarization time (QTc) during normal conduction in the HOCM patients. This different response might be explained by the down-regulation of I_{to} in the HOCM patients existing already at baseline [54]. The down-regulation of I_{to} is associated with the development of *cardiac memory* in the structurally normal heart, see below [51].

During ventricular pacing, however, the repolarization time (JTc) was significantly shorter than during post-pacing normal conduction, a phenomenon that was also observed in the control group (analyzed in Study II).

Cardiac memory and the WPW syndrome

Based on T-wave analysis, we observed ECG signs of *cardiac memory* in almost all (98%) of 125 WPW patients ablated due to a PS accessory pathway (Study IV). The two patients who did not show *cardiac memory* both had documented intermittent preexcitation prior to ablation. Previous ECG-based studies of WPW ablation had shown signs of *cardiac memory* to a varying extent; Table 7. Some studies included patients with different accessory pathway locations and concluded that the occurrence of *cardiac memory* depended on the pathway site [8, 9, 13]. We hypothesized that any altered activation sequence would result in the development of *cardiac memory* according to its definition, no matter whether it was caused by ventricular pacing or preexcitation via an accessory pathway. Consequently, we assumed that the previously reported difference in the occurrence of *cardiac memory* did not depend on the accessory pathway site but was due to limitations inherent to ECG. We therefore used VCG to compare repolarization changes after the ablation of overt PS and LL accessory pathways and concluded that *cardiac memory* was present, independent of pathway site (Study V).

Although the study of PS accessory pathways (Study IV) was retrospective with its known limitations, it included a far larger number of patients and a more homogeneous group than previous studies. We evaluated T-wave inversions in the frontal plane leads II, aVF and III, since these changes had previously

Table 7. ECG signs of *cardiac memory* after the ablation of accessory pathways (AP) in previous reports.

Author	n	T-wave changes post ablation		Follow-up	Memory dissipation
		Overt AP	Concealed AP		
Kalbfleisch [8]	45	22* / 29 (76%)	0 / 16 (0%)	1+3 months	3 months
Poole [10]	7	7 / 7 (100%)	0 / 2 (0%)	1+2+6 months	1 month
Wood [9]	37†	9 / 19 (47%)	0 / 6 (0%)	4 days-16 weeks	4 weeks (2 pts) >5 weeks (2 pts)
Helguera [11]	51	23 / 24 (96%)	2‡ / 27 (7,4%)	6 weeks	6 weeks
Geller [13]	90	38§ / 64 (59%)	0 / 26	1+3 months	1 month (70%) 3 months (all)
Study IV	125	123/125 (98%)	N/A	≤ 12 months	~ 3 months (~ 90%)

* Another 4 patients had T-wave changes the day after ablation
†12 AVNRT with no T-wave changes
‡ No data regarding the kind of T-wave changes (inversion or peaking)
§ Another 3 patients had T-wave changes the day after ablation
Reprinted from Study IV with permission from the publisher

been reported to occur after the ablation of PS accessory pathways [10, 11]. Other studies including accessory pathways with different locations assessed both T-wave inversion and peaking [8, 11, 13]. This should be borne in mind when comparing studies in Table 7.

Some authors have emphasized that the direction of the post-ablation T-wave vector was similar to the direction of the delta-wave vector [8, 10, 11, 13], while others have stated that it was similar to the direction of the main preexcited QRS vector [55]. According to our results, both are equally correct (Study IV). Furthermore, the prospective VCG study (Study V) showed a moderate to strong correlation between the angle of the maximum T vector post ablation and the angle of the preexcited maximum QRS vector.

A correlation between the degree of preexcitation measured as QRS duration prior to ablation and the extent of post-ablation T-wave changes has previously been reported [8, 9, 13]. No correlation of this kind was confirmed in our study. This could be explained by the use of different methods for measuring the degree of T-wave changes. We used the number of inferior leads (II, aVF, III) with T-wave inversion after ablation as an estimate of the degree of cardiac memory, whereas others have graded the T-wave changes as none, mild or marked [8, 13] or have divided the patients into one group with T-wave changes and another without them [9].

In a few patients, T-wave inversions did not occur until the day after ablation. This phenomenon was also reported by Kalbfleisch et al., who found 14% [8], and Geller et al., who found 5% [13], compared with our 11% of patients with the delayed onset of T-wave changes. The reason for this is unclear, but it may be due to methodological and/or biological factors, such as a change in the position of the heart due to several hours in the supine position during and after the ablation procedure.

When comparing *cardiac memory* after the ablation of accessory pathways in different locations (Study V), we found T-wave inversions on ECG after the ablation of PS but not after the ablation of LL accessory pathways. The VCG analysis, on the other hand, revealed T-vector changes in the horizontal / transverse plane (high maximum T-vector azimuth values) after the ablation of LL and in the vertical direction (high T-vector elevation values) after the ablation of PS accessory pathways. This confirmed our hypothesis that the development of *cardiac memory* is independent of the accessory pathway site and probably explains why ECG-based studies of the post-ablation T wave report signs of *cardiac memory* in a varying percentage of patients with different accessory pathways.

QRS-T angles in the frontal and horizontal planes measured from 12-lead ECGs were analyzed by Helguera et al. They only found changes in the frontal plane, although they included patients with both right- and left-sided accessory pathways [11]. Herweg et al. analyzed the QRS and T vector and the QRS-T angle in the frontal plane from ECG and concluded that *cardiac memory* was more pronounced in patients with posterior accessory pathways [55].

Our results are, however, in line with previous studies of repolarization changes *during* preexcitation and after the ablation of overt accessory pathways using body surface QRST time integrals. These are achieved by integrating each lead over the time interval from the beginning of the QRS complex to the end of the T wave; (unit: mV • ms). Abnormal QRST values were found before and 1 day, but not 1 week, after ablation in leads reflecting the frontal plane in right-sided accessory pathways and in leads reflecting the horizontal plane in left-sided accessory pathways [12, 56]. Studies of QRST time integrals have also demonstrated that repolarization abnormalities do not exist in patients with concealed accessory pathways [12, 56, 57]. Analysis of the QRST time integral, however, is performed on the assumption that it is independent of activation sequence. *Cardiac memory*, on the other hand, is crucially dependent on activation sequence and these results therefore require confirmation.

Another method of analysis is the spatial ventricular gradient (VG) assessed by the VCG. Each of the Frank orthogonal leads (X, Y, Z) was integrated over the time interval from the beginning of the QRS complex to the end of the T wave; (unit: mV • ms). The spatial VG was

defined as the resultant vector and expressed in terms of amplitude, azimuth and elevation. Also for this method, is the assumption that it is independent of activation sequence. The spatial VG was used by Sugino et al. to study repolarization abnormalities before, one day and one week after the ablation of accessory pathways. They found an anterior deviation of the spatial VG in patients with an overt left-sided accessory pathway and a superior deviation in patients with an overt right-sided accessory pathway [58]. This is in line with our results obtained by pure repolarization analysis reflected by the T-vector loop and its maximum vector.

The disappearance of *cardiac memory* after WPW ablation has been reported to take place between 4 weeks and 3 months in previous studies [8-11, 13]; Table 7. In Study IV, we found normalization in about 90% of available ECGs after 3 months, but changes persisted in some patients for up to more than 6 months. Study V showed normalization of the VCG in 82% of the patients within 3-4 weeks. In the pacing model of *cardiac memory*, the extent of repolarization changes and the time of their disappearance depended on the duration of the previous altered activation sequence [3, 14]. Since *cardiac memory* is regarded as a general concept, the same relationship was also supposed to apply to WPW patients. We therefore compared 2 equally sized groups of all patients aged < 20 and > 50 years, on the assumption of a life-long preexcitation. The degree of *cardiac memory* was assessed as the number of inferior leads (II, aVF, III) with T-wave inversions. We found a significantly "stronger" memory in the higher age group one day after the ablation procedure ($p < 0.01$).

Methodology aspects

Previous studies of *cardiac memory* in humans have mainly used the 12-lead ECG, either to identify T-wave amplitude changes or to calculate QRS and T vectors in the frontal and horizontal planes [11, 55]. In the studies of WPW patients, some groups also have used the QRST time integral [12, 56, 57] and the spatial VG [58, 59]. In the dog model,VCG in the frontal plane has been used.

Since depolarization and repolarization in the heart are spread in a 3-dimensional pattern, we chose to use the spatial VCG for the characterization of *cardiac memory*. The spatial QRS and T loops are assumed to contain all the information about electrical activity in the ventricles [60]. When the 3-dimensional loop is projected onto a 2-dimensional plane or onto a single lead, information will inevitably be lost. We therefore analyzed the amplitude and location of the maximum vector in space and not in separate planes.

It is clear that *cardiac memory* represents fairly pronounced repolarization changes and the fact that repolarization heterogeneity may lead to arrhythmias is also well known. In spite of this, there is no ideal and generally accepted method for non-invasive assessments of "global" repolarization in the human heart. The measurement of QT dispersion is controversial, the main arguments being whether or not the QT interval on ECG reflects local repolarization and whether the measurements are affected by information redundancy due to the projection on single leads creating "false dispersion". There are also problems with measurement precision, since especially the end of the T wave might be hard to identify, and there is also a considerable time-dependent variability [61].

A new approach to measurements of repolarization heterogeneity is the analysis of the spatial T-vector loop morphology. Several parameters have been proposed. Usually, one parameter describing the planarity of the loop (in this thesis Tavplan) and one describing the symmetry or roundness of the loop (in this thesis Tegenv) are used.

A loss of planarity and an increase in the roundness of the spatial T-vector loop have been observed in both post-myocardial infarction patients [43, 60] and patients with the long QT syndrome [60], as well as during ischemia [40, 41]. An increase in QT dispersion has been associated with a wider [40, 43] and less planar T-vector loop [43]. It has also been reported that QT dispersion was smallest for narrow, tall T loops and largest for wide, small T loops [44]. Clinically, it has been shown that abnormalities in T-vector loop morphology are a risk factor for cardiac events in the elderly [62].

A third parameter that is used is some kind of area (in this thesis the "3-dimensional" area, Tarea). A correlation between increased "3-dimensional" area, Tarea and ischemia has been reported [40, 41].

The VCG parameters maximum T-vector amplitude and the loop parameter Tarea detected repolarization changes within one day after the onset of right ventricular endocardial pacing at physiologic rates, which was before T-wave inversions were seen on ECG in most patients.

Another advantage of VCG compared with ECG is that it more easily enables the quantification of repolarization changes.

All ECG and VCG recordings were performed with the patient in the supine position to avoid changes in the position of the heart in relation to the recording electrodes and after at least 5 minutes' rest to allow for the rate adaptation of repolarization [45, 46].

The time-dependent variations in repeated VCG recordings were ≤ 10 º on average in both the internal and external control group (azimuth: 7 ± 5 º and 10 ± 4 º respectively; elevation: 4 ± 3 º and 5 ± 2 º respectively).

Mechanisms of cardiac memory

Our results imply that *cardiac memory* might be an adaptation mechanism of the heart. An altered activation sequence, such as ventricular pacing, results in a progressive change in repolarization. If the activation sequence normalizes, i.e. at the cessation of ventricular pacing or the ablation of an accessory pathway, the repolarization will again slowly adapt. The adaptation or electrical remodeling thus occurs *during* the altered activation sequence, but it will not be evident on the ECG until normal activation is re-established.
This is in line with observations before and after the ablation of overt accessory pathways in WPW patients. The prolongation of the activation-recovery interval (ARI), which correlates to APD, over the preexcited region both before and just after WPW ablation has been demonstrated from body surface mapping [63], as well as from epicardial measurements [64]. One week after ablation, the ARI had decreased. There was also an inverse relationship between the activation time (AT) and ARI, which was stronger the day before ablation and one week after ablation compared with 1 day after ablation [63].
Similar behavior was shown in the short-term *in vitro* study of Langendorff-perfused rabbit hearts. During continuous atrial pacing, there was an inverse relationship between AT and APD. After abruptly switching the pacing site from the atrium to the ventricular apex, a marked change in AT occurred but almost no change in APD and consequently the inverse relationship was lost. During the following continuous ventricular pacing, the APD changed progressively and the initial inverse relationship was re-established. After switching back to atrial pacing, the same phenomenon occurred [52]. This inverse relationship between AT and APD may synchronize ventricular repolarization and might thus have an anti-arrhythmic effect [52]. This implies that the adaptation mechanism of *cardiac memory* might be anti-arrhythmic.

Measurements on myocardial strips from dogs paced from the left ventricular epicardium for 3 weeks (long-term *cardiac memory*) showed the prolongation of epicardial and endocardial APDs, but no change in midmyocardial cells [18]. Normally, APD of the epicardium is shorter than APD of the endocardium, but, after the development of long-term *cardiac memory*, the APD of epicardium and endocardium became more similar [18]. The changes in APD in different layers of the myocardium alter the transmural repolarization gradient.

In general, the depolarization of the ventricles is mainly a "global" event with the rapid spread of a depolarization wave. The repolarization of the ventricles, on the other hand, is probably a more "local" event depending on properties of myocytes in the local area. The T wave is mainly the net result of inward Ca^{2+} currents and outward K^{+} currents of the APs of the ventricular myocytes and depends on regional and transmural differences in the APs [65].
Whether the T wave is mainly due to transmural or regional differences in repolarization has not been fully clarified.

Potential mechanisms of *cardiac memory* have been studied in intact animal models, as well

as in isolated hearts, isolated tissues and single cells [1].

Ventricular pacing leads to an altered activation sequence, which in turn changes the stress/strain relationships in the myocardium [20, 66, 67]. The change in stress/strain relationships increased the release of angiotensin II in cardiac cell cultures [68, 69]. In intact dogs, ACE inhibition and angiotensin II type-1-receptor blockade both inhibited the initiation of *cardiac memory* (short-term memory) [20] but did not affect long-term *cardiac memory* [1]. The incubation of canine epicardial ventricular myocytes with angiotensin II for hours/days resulted in changes in the AP notch and I_{to} consistent with the development of *cardiac memory* [70], see below.

The transient outward current, I_{to}, which is responsible for the phase 1 notch in the AP, probably plays an important role in the development of *cardiac memory*. The development of short-term *cardiac memory* (3x20 minutes of right ventricular epicardial pacing) in anesthetized dogs was prevented by the I_{to} blocker 4-aminopyridine [21]. In another study of ventricular subepicardial and subendocardial slabs from dogs, the phase 1 notch in epicardial cells decreased during ventricular pacing, as well as after the administration of 4-aminopyridine. When treated with 4-aminopyridine, epicardial cells behaved like endocardial cells and *cardiac memory* did not develop [22].

Young dogs (< 2months) do not express I_{to} and *cardiac memory* was not inducible. With increasing age, the ability to induce *cardiac memory* gradually increased in parallel with the evolution of a phase 1 notch of the AP [71].

In left ventricular epicardially paced dogs, long-term *cardiac memory* (3 weeks of ventricular pacing) was associated with prolonged APD and a smaller phase 1 notch in epicardial myocytes. In addition, the kinetics of I_{to} changed, resulting in activation at a more positive potential and a more than 20-fold prolongation of the time for recovery from inactivation. A down-regulation of the gene encoding for the K^+ channel mainly responsible for I_{to} was found as well, indicating that new protein synthesis might be involved in the development of long-term *cardiac memory* [51]. It has also been shown that cycloheximide, which inhibits protein synthesis, diminished *cardiac memory* development during 3 weeks of left ventricular epicardial pacing in intact dogs [18]. The changes in epicardial but not endocardial myocytes described above will alter the transmural repolarization gradient and as a result probably also the T wave.

Although I_{to} appears to play an important role in *cardiac memory*, there are obviously other less investigated mechanisms.

The L-type Ca^{2+} channel, which contributes to the AP plateau, was activated at a more positive membrane potential and remained open for a longer time in canine epicardial myocytes after the induction of long-term *cardiac memory*. The same study showed that the evolution of both short- and long-term *cardiac memory* was attenuated by blockers of the L-type Ca^{2+} channel [72].

Another mechanism, involving the coupling between cells, is the change in gap junctions. During long-term *cardiac memory*, the density of the gap junction protein Cx43 was reduced and it was also redistributed from the ends of the myocytes to the lateral surfaces [73]. Interestingly, a preliminary report showed that 3 months of ventricular endocardial pacing in HOCM patients was associated with an increase in Cx43 [74]. There are also indications that the rapidly activating delayed rectifier I_{Kr} is involved in *cardiac memory* [75].

Implications

Cardiac memory reflects fairly pronounced repolarization changes, but until recently it was mainly regarded as a differential diagnostic problem. Now the question of whether *cardiac memory* might be pro-arrhythmic or anti-arrhythmic is being raised.

The differential diagnostic problem of distinguishing between *cardiac memory* T-wave changes and ischemic T-wave changes was recognized back in the 1970s in the setting of intermittent left bundle branch block [5, 6]. Since both WPW ablation and pacemaker therapy are common treatments today, it is important for the medical profession to be aware of the nature of these ECG changes. In WPW patients, ECG changes may persist for several months after the

ablation procedure and pacemaker patients who are only intermittently ventricular paced might manifest T-wave inversions in all normally conducted beats for the rest of their lives. An algorithm that uses the direction of the frontal plane T-wave vector to differentiate between pacing-induced *cardiac memory* and ischemic T-wave changes has been described [76].

There is evidence of an interaction between *cardiac memory* and different drugs in dogs, but it is not known whether this is also valid for humans. As mentioned above, ACE inhibitors and angiotensin II type-1-receptor blockers both inhibited the initiation of *cardiac memory* (short-term *cardiac memory*) [20] and L-type Ca^{2+} channel blockers attenuated both short- and long-term *cardiac memory* [72]. The anti-arrhythmic drug quinidine prolonged repolarization (QT interval) and suppressed the development of *cardiac memory*. However, the effect of quinidine in prolonging the QT interval was lost during *cardiac memory* [50]. It is therefore possible that *cardiac memory* might modulate the effect of anti-arrhythmic drugs in pacemaker patients. According to the Swedish pacemaker registry, approximately 30-40 % of patients with the sick sinus syndrome also have supraventricular tachycardias, mostly atrial fibrillation, and might receive drug therapy.

Until recently, pacemaker treatment was regarded as a benign intervention. However, in humans, signs of diastolic but not systolic dysfunction were observed in parallel with ECG signs of *cardiac memory* after 1 week of ventricular pacing [17]. Today, diastolic dysfunction is an increasingly recognized cause of heart failure and there was a relationship between the extent of ventricular pacing and the risk of heart failure hospitalizations both in the MOST trial [77], in which > 80% of the patients were in New York Heart Association class I or II at baseline, and in the DAVID study of patients with impaired ventricular function already at baseline (ejection fraction ≤ 40%) [78]. This detrimental effect was tentatively related to increased heart rate, decreased AV interval, or pacing-induced ventricular desynchronization, or a combination [78]; the possibility of impaired diastolic function should, however, also be kept in mind. A common denominator for *cardiac memory* and both ischemic and dilated cardiomyopathies is a down-regulation and redistribution of gap junctions in cardiac myocytes [79].

Whether possible mechanical disadvantages of pacemaker treatment are associated with *cardiac memory,* or whether they are just parallel phenomena still has to be investigated. Despite this, we found indications that repolarization changes related to cardiac memory might be unfavorable. The increase in the repolarization time (QTc) compared with baseline values may thus imply an increased risk of arrhythmias. Additionally, the observed decrease in Tegenv (more circular T loop) and increase in Tavplan (more bulgy T loop) are possible signs of increased repolarization heterogeneity. Importantly, however, these changes are seen when *abruptly switching from > 90% ventricular pacing* for days to weeks to normal conduction. *During* continuous ventricular pacing, on the other hand, there appeared to be an adaptation over days to weeks to the new activation sequence with a successively shorter repolarization time. Whether the observed repolarization changes translate into an increased propensity for ventricular arrhythmias remains to be established. There is also uncertainty about what happens when repeated switching between ventricular pacing and normal conduction takes place. If *cardiac memory* is an adaptation mechanism of the heart, aimed at stabilizing repolarization, switching between different activation patterns should be avoided. Consequently, in pacemaker patients, if ventricular pacing cannot be avoided, it might electrophysiologically be better to pace the ventricle continuously rather than switching between pacing and no pacing.

In patients with HOCM, a somewhat different response to ventricular pacing was observed. No prolongation of repolarization time was observed after the cessation of ventricular pacing, as was seen in the structurally normal hearts. This may be related to I_{to}, which appears to be crucial in the development of cardiac memory. I_{to} is down-regulated in HOCM patients or actually in myocardial hypertrophy independent of cause, where a more fetal phenotype is expressed [54].

Questions have also been raised about whether there is *cardiac memory* in the atria as well and, if so, whether there is any association with atrial fibrillation.

Limitations

The number of patients in Studies I and II was fairly small and their age and clinical background were heterogeneous. Despite this, the temporal pattern of memory development was very consistent. However, conclusions relating to any influence by different drugs and unipolar versus bipolar pacing could not be reached.
In a few patients, atrial fibrillation attenuated the development of *cardiac memory*. Furthermore, although the pacemaker log is a valuable tool, it cannot differentiate between complete or incomplete stimulation of the ventricle (fusion or pseudo-fusion). The latter might lead to the reduced development of *cardiac memory*, while frequent ventricular extra-systoles would have the opposite effect. In fact, memory development might have occurred even more rapidly if the ventricle in all patients had been fully preexcited 100% of the time.

In Study II and III, the QT interval was measured, which is a well-recognized challenge. We adhered to standard criteria and only one person measured the QT intervals in order to minimize inter-observer variability.

The possible negative and positive effects on ventricular repolarization observed in Studies II and III in relation to *cardiac memory* development might be linked only by inference to an increased or decreased risk of arrhythmias. Effects on the prevalence of ventricular arrhythmias and on even harder end-points, such as sudden cardiac death, have not been presented. However, both animal and human data strongly suggest that the magnitude of repolarization changes observed in this study might be clinically relevant [80-84].

Study IV has the known limitations of a retrospective study, but the patient group was large and homogeneous according to the accessory pathway location (PS). The ECG analysis was qualitative and not quantitative and focused on the frontal plane (leads II, aVF, III). As shown in Study I, the frontal plane is not sufficient to detect repolarization changes in all directions. In spite of this, our results were consistent within the group and with previous observations. Study V also confirmed that *cardiac memory* due to PS accessory pathways is mainly expressed in the vertical direction. Further, T-wave inversion solely in lead III is within normal limits and on its own has limited value for evaluating *cardiac memory*. Finally, there might be a bias in the later recordings, since patients with ECG changes might be more likely to have repeated ECGs performed.

In Study V, which is an interim report, the number of patients was limited, especially in the LL and concealed group. This affects the statistical power, but significant changes were still obtained, supporting our hypothesis. The different groups (PS or LL) were defined according to the pre-ablation ECG, which is dependent on both the AP location and the rotation of the heart around its long axis.

Cardiac memory – future speculation

Even though a great deal of research has been performed in the last decade on the mechanisms of cardiac memory, there are still many more questions to explore.

- What is the first thing that happens after the activation sequence has changed? We are now investigating the cardiac release of different hormones after rapid pacing for 30 minutes in humans.
- What is the importance of angiotensin II in relation to *cardiac memory*? Is it just a signal molecule or is *cardiac memory* the beginning of impaired diastolic function?
- Is the change in the expression and distribution of gap junctions crucial for the development of *cardiac memory* or is it just a parallel phenomenon? There is no question that gap junctions are involved in the spread of the depolarization among myocytes.
- Is there a coupling between electrical and mechanical remodeling in the human heart? Although the influx of Ca^{2+} into the cardiac myocyte is dependent on the AP, it still remains to be investigated whether

electrical remodeling (*cardiac memory*) results in mechanical remodeling or whether it is just a parallel phenomenon. We are now investigating WPW patients before and after ablation, not only with ECG and VCG but also with echocardiography, including tissue Doppler imaging.

- Should ventricular pacing be performed in a location other than the right ventricular apex? For mechanical reasons, it is probably better with an activation pattern that is more like the normal activation sequence. For electrical reasons, we still do not know. Hypothetically, it might be that different pacing sites, including endocardial or epicardial sites, have pro-arrhythmic or anti-arrhythmic qualities, especially in the structurally and functionally abnormal heart.
- What about cardiac resynchronization therapy? As yet, there are no reports on *cardiac memory* when ventricular pacing is performed from two sites at the same time, besides one endocardial and one epicardial site.
- Are there interactions in both directions between *cardiac memory* and anti-arrhythmic drugs? There is no question that there are interactions, at least in dogs. Theoretically, *cardiac memory* induced by ventricular pacing, LBBB, ventricular extra-systoles or tachycardia may interact with drugs in both a positive or negative manner. It could well be that the currently fairly unpredictable behavior of some anti-arrhythmic drugs is the result of interaction with *cardiac memory*. With more knowledge in this field, the interactions might be turned into an advantage.
- What is the difference between short- and long-term *cardiac memory*? To date, all the studies have investigated either short- or long-term *cardiac memory*, although the time frames are not clear. How short-term *cardiac memory* is turned into long-term *cardiac memory* still needs exploration. The result might affect the point at which a possible intervention with *cardiac memory* should be performed.
- Is *cardiac memory* present in the atrium? Although there are differences between atrial and ventricular myocytes and their APs, their function is principally the same. So, there is presumably an atrial *cardiac memory* and some groups are also doing research in this field. Whether or not this this will lead to greater understanding and new therapies for atrial fibrillation, the most common arrhythmia, is still a dream of the future.

CONCLUSIONS

- *Cardiac memory* is a form of electrical remodeling induced by altered ventricular activation where the T vector during normal activation follows the previously altered QRS vector in both human models studied in this thesis.

- After the initiation of right ventricular endocardial pacing in humans, repolarization changes appeared within 24 hours and *cardiac memory* was fully developed within 1 week. *Cardiac memory* was then retained in proportion to the percentage of ventricular pacing but disappeared within 4 weeks after the complete cessation of pacing.

- The repolarization changes related to pacing-induced *cardiac memory* were different in patients with hypertrophic obstructive cardiomyopathy compared with control patients.

- *Cardiac memory* was present in all patients after accessory pathway ablation in patients with overt WPW syndrome. The repolarization changes were mainly expressed in the transverse plane after the ablation of a left lateral accessory pathway and mainly in the vertical direction after the ablation of a posteroseptal accessory pathway. The dissipation of *cardiac memory* after WPW ablation usually occurred within 3 months.

- *Cardiac memory* is probably part of a response mechanism of the heart, where repolarization adapts to an altered depolarization, presumably in a stabilizing "anti-arrhythmic" direction. It is worth noting that *abrupt* switches between different activation sequences might lead to unfavorable repolarization changes.

- The analysis of the spatial VCG in 3 dimensions, including T-vector loop morphology, is a useful method for detecting repolarization changes.

Acknowledgements

I wish to express my sincere gratitude to all those who have supported and helped me and thus made this thesis possible. In particular I wish to thank:

Professor *Lennart Bergfeldt*, my supervisor, for excellent scientific guidance and great support. You have a profound knowledge of cardiac arrhythmias, which you are always willing to share and explain with great enthusiasm and in an outstanding pedagogic manner. Thank you also for taking me to New York visiting professor Rosen and his laboratory and the Guggenheim museum.

Professor *Lars Rydén*, former Chairman of the Cardiology Department, for giving me the opportunity to come to Karolinska University Hospital and be part of the excellent research environment you have created, and for great support during my PhD work.

Associate Professor *Cecilia Linde*, Chairman of the Cardiology Department and co-author, for providing me with the time to do scientific work and also for valuable input on manuscripts.

Fredrik Gadler, Head of the Pacemaker Section and co-author, for support and valuable input on manuscripts.

Professor *Michael R. Rosen* at Columbia University in New York, co-author, for sharing your tremendous knowledge on cardiac memory and valuable input on manuscripts. Thank you also for your generous guidance through your laboratory. You really are "Mr. Cardiac Memory".

Associate Professor *John Pernow*, for your support in planning of the dissertation and for clinical guidance on the CCU.

Gunilla Lundahl, co-author and former employee at Ortivus AB, for help with understanding and calculating T-vector loop parameters and valuable input on manuscripts.

Karolina Nowinski colleague and co-author, for input on posters and general advice on being a PhD-student mixed with friendly chats.

My co-authors, Associate Professor *Nils Edvardsson, Maria Aunes-Jansson*, late *Leon Lurje*, *Dritan Poçi* and *Birgitta Johansson* at Sahlgrenska University Hospital in Gothenburg and Associate Professor *Jonas Schwieler* at Karolinska University Hospital.

Eva Wallgren, the master of the MIDA system, for recording of a tremendous number of VCGs and ECGs and for taking care of the study patients. You are always friendly and in a good mood. And not the least, I'd like to thank you for putting this thesis with all its pictures together and calmly trying to convince me that it will be finished in time.

Birgitta Nordlöf, for recording hundreds of ECGs and VCGs and arranging my patient data in perfect records. Your patience in measuring all ECGs on the digitizing table was amazing.

Aigars Rubulis for interesting discussions about the T-vector loop and its morphology.

Anna Norhammar, *Christina Jarnert*, *Inga Thrainsdottir* and all other colleagues at the Cardiology Department at Karolinska University Hospital.

David Ersgård for ECG/VCG recordings and help with several posters, *Kerstin Höglund* for helping me with my first poster, and *Marian Lettosunti*, *Helena Karlsson* and *Pia Oblack* for help with study patients.

Mats Andersson for mastering the digitizing table and its old computer, including writing programs for it.

Elisabeth Berg for statistical advice and for making statistics comprehensible.

Britta Nyström and *Lotta Backman* at Sahlgrenska University Hospital for taking care of the study patients in Gothenburg.

Frieder Braunschweig, *Hamid Bastani* and the staff of the EP lab for help with study patients and clinical guidance.

Magnus Mossfeldt for solving all my computer problems.

Jeanette Kliger for linguistic help.

Kirsti Wallin, Helena Kagger and *Berith Haavik* for help with practical matters.

Elisabeth Nordeman for practical help and nice chats.

My close friends *Karin Fors*, *Karin Mattson*, *Erika Bergner, Gunbritt Skog, Lisbeth Pettersson,* my sewing mates *Anna Eelde* and *Anna Fergin* and many more, for support, encouragement, and a lot of fun.

My mother *Berit*, my brother *Urban*, my sister-in-law *Karin* and my wonderful nephew *Nils,* for love, support and encouragement.

Per for all support, care, encouragement and a tremendous number of long distance calls.

And last but not least, *all patients* who willingly took part in the studies and made this thesis possible.

This work has been supported by grants from the Swedish Heart-Lung Foundation, the Stockholm County Council, the Karolinska Institute, Sahlgrenska University Hospital and the Gothenburg Society of Medicine.

The MIDA 1000 system was a loan from Ortivus AB, Täby, Sweden.

REFERENCES

1. Rosen MR. The electrocardiogram 100 years later: electrical insights into molecular messages. ***Circulation.*** Oct 22 2002;106(17):2173-2179.

2. Chatterjee K, Harris AM, Davies JG, et al. T-wave changes after artificial pacing. ***Lancet.*** Apr 12 1969;1(7598):759-760.

3. Chatterjee K, Harris A, Davies G, et al. Electrocardiographic changes subsequent to artificial ventricular depolarization. ***Br Heart J.*** Nov 1969;31(6):770-779.

4. Kernohan RJ. Post-paroxysmal tachycardia syndrome. ***Br Heart J.*** Nov 1969;31(6):803-806.

5. Engel TR, Shah R, DePodesta LA, et al. T-wave abnormalities of intermittent left bundle-branch block. ***Ann Intern Med.*** Aug 1978;89(2):204-206.

6. Denes P, Pick A, Miller RH, et al. A characteristic precordial repolarization abnormality with intermittent left bundle-branch block. ***Ann Intern Med.*** Jul 1978;89(1):55-57.

7. Nicolai P, Medvedowsky JL, Delaage M, et al. Wolff-Parkinson-White syndrome: T wave abnormalities during normal pathway conduction. ***J Electrocardiol.*** Jul 1981;14(3):295-300.

8. Kalbfleisch SJ, Sousa J, el-Atassi R, et al. Repolarization abnormalities after catheter ablation of accessory atrioventricular connections with radiofrequency current. ***J Am Coll Cardiol.*** Dec 1991;18(7):1761-1766.

9. Wood MA, DiMarco JP, Haines DE. Electrocardiographic abnormalities after radiofrequency catheter ablation of accessory bypass tracts in the Wolff-Parkinson-White syndrome. ***Am J Cardiol.*** Jul 15 1992;70(2):200-204.

10. Poole JE, Bardy GH. Further evidence supporting the concept of T-wave memory: observation in patients having undergone high-energy direct current catheter ablation of the Wolff-Parkinson-White syndrome. ***Eur Heart J.*** Jun 1992;13(6):801-807.

11. Helguera ME, Pinski SL, Sterba R, et al. Memory T waves after radiofrequency catheter ablation of accessory atrioventricular connections in Wolff-Parkinson-White syndrome. ***J Electrocardiol.*** Jul 1994;27(3):243-249.

12. Tomita Y, Hirai M, Yanagawa T, et al. Body surface distribution of significant changes in QRST time-integral values after radiofrequency catheter ablation in patients with Wolff-Parkinson-White syndrome. ***Am J Cardiol.*** Jan 1 1996;77(1):59-63.

13. Geller JC, Carlson MD, Goette A, et al. Persistent T-wave changes after radiofrequency catheter ablation of an accessory connection (Wolff-parkinson-white syndrome) are caused by "cardiac memory". ***Am Heart J.*** Nov 1999;138(5 Pt 1):987-993.

14. Rosenbaum MB, Blanco HH, Elizari MV, et al. Electrotonic modulation of the T wave and cardiac memory. ***Am J Cardiol.*** Aug 1982;50(2):213-222.

15. Rosen MR, Cohen IS, Danilo P, Jr., et al. The heart remembers. ***Cardiovasc Res.*** Dec 1998;40(3):469-482.

16. Kandel ER. Genes, nerve cells, and the remembrance of things past. ***J Neuropsychiatry Clin Neurosci.*** Spring 1989;1(2):103-125.

17. Alessandrini RS, McPherson DD, Kadish AH, et al. Cardiac memory: a mechanical and electrical phenomenon. ***Am J Physiol.*** Apr 1997;272(4 Pt 2):H1952-1959.

18. Shvilkin A, Danilo P, Jr., Wang J, et al. Evolution and resolution of long-term cardiac memory. ***Circulation.*** May 12 1998;97(18):1810-1817.

19. Katz AM. T Wave "Memory": Possible Causal Relationship to Stress-Induced Changes in Cardiac Ion Channels? ***J Cardiovasc Electrophysiol.*** Apr 1992;3(2):150-159.

20. Ricard P, Danilo P, Jr., Cohen IS, et al. A role for the renin-angiotensin system in the evolution of cardiac memory. ***J Cardiovasc Electrophysiol.*** Apr 1999;10(4):545-551.

21. del Balzo U, Rosen MR. T wave changes persisting after ventricular pacing in canine heart are altered by 4-aminopyridine but not by lidocaine. Implications with respect to phenomenon of cardiac 'memory'. ***Circulation.*** Apr 1992;85(4):1464-1472.

22. Geller JC, Rosen MR. Persistent T-wave changes after alteration of the ventricular activation sequence. New insights into cellular mechanisms of 'cardiac memory'. ***Circulation.*** Oct 1993;88(4 Pt 1):1811-1819.

23. Jalife J, Delmar M, Davidenko JM, et al. ***Basic Cardiac Electrophysiology For The Clinician***. Armonk, NY: Futura Publishing Company, Inc.; 1999.

24. Bers DM. ***Cardiac Calcium Channels.*** *In: Zipes DP, Jalife J, eds. Cardiac Electrophysiology. From Cell to bedside.* 4th ed. Philadelphia, PA: WB Saunders; 2004:10-18.

25. Chen X, Houser SR. ***Pharmacology of the L-Type and T-Type Channels in the Heart.*** *In: Zipes DP, Jalife J, eds. Cardiac Electrophysiology. From Cell to bedside.* 4th ed. Philadelphia, PA: WB Saunders; 2004:133-142.

26. Oudit GY, Ramirez RJ, Backx H. ***Voltage-regulated Potassium Channels.*** *In: Zipes DP, Jalife J, eds. Cardiac Electrophysiology. From Cell to bedside.* 4th ed. Philadelphia, PA: WB Saunders; 2004:19-32.

27. Sanguinetti MC, Tristani-Firouzi M. ***Gating of Cardiac Delayed Rectifier K^+ Channels.*** *In: Zipes DP, Jalife J, eds. Cardiac Electrophysiology. From Cell to bedside.* 4th ed. Philadelphia, PA: WB Saunders; 2004:88-95.

28. Nerbonne JM. ***Heterogeneous Expression of Potassium Channels in the Mammalian Myocardium.*** *In: Zipes DP, Jalife J, eds. Cardiac Electrophysiology. From Cell to bedside.* 4th ed. Philadelphia, PA: WB Saunders; 2004:169-180.

29. Meissner G. ***Sarcoplasmic Reticulum Ion Channels.*** *In: Zipes DP, Jalife J, eds. Cardiac Electrophysiology. From Cell to bedside.* 4th ed. Philadelphia, PA: WB Saunders; 2004:51-58.

30. Delmar M, Duffy HS, Sorgen PL, et al. ***Molecular Organization and Regulation of the Cardiac Gap Junction Channel Connexin 43.*** *In: Zipes DP, Jalife J, eds. Cardiac Electrophysiology. From Cell to bedside.* 4th ed. Philadelphia, PA: WB Saunders; 2004:66-76.

31. Moreno AP, Hayrapetyan V, Zhong G, et al. ***Homomeric and Heteromeric Gap Junctions.*** *In: Zipes DP, Jalife J, eds. Cardiac Electrophysiology. From Cell to bedside.* 4th ed. Philadelphia, PA: WB Saunders; 2004:120-126.

32. Saffitz JE, Lerner DL, Yamada KA. ***Gap Junction Distribution and Regulation in the Heart.*** *In: Zipes DP, Jalife J, eds. Cardiac Electrophysiology. From Cell to bedside.* 4th ed. Philadelphia, PA: WB Saunders; 2004:181-191.

33. Rohr S, Kucera JP. ***Cardiac Tissue Architecture Determines Velocity and Safety of Propagation.*** *In: Zipes DP, Jalife J, eds. Cardiac Electrophysiology. From Cell to bedside.* 4th ed. Philadelphia, PA: WB Saunders; 2004:222-231.

34. Antzelevitch C. ***Drug-induced Channelopathies.*** *In: Zipes DP, Jalife J, eds. Cardiac Electrophysiology. From Cell to bedside.* 4th ed. Philadelphia, PA: WB Saunders; 2004:151-157.

35. MacFarlane PW. ***The Coming of Age of Electrocardiology.*** *In: Macfarlane PW, Lawrie TDV,eds. Comprehensive Electrocardiology: Theory and Practice in Health and Disease, Volume 1.* New York: Pergamon Press; 1989:3-40.

36. Anyukhovsky EP, Sosunov EA, Feinmark SJ, et al. Effects of quinidine on repolarization in canine epicardium, midmyocardium, and endocardium: II. In vivo study. ***Circulation.*** Dec 2 1997;96(11):4019-4026.

37. Wartak J. ***Simplified Vectorcardiography***. Philadelphia: J. B. Lippincott Company; 1970.

38. Chou TC, Helm RA, Kaplan S. ***Clinical Vectorcardiography***. 2nd ed. New York: Grune & Stratton; 1974.

39. Frank E. An accurate, clinically practical system for spatial vectorcardiography. ***Circulation.*** May 1956;13(5):737-749.

40. Nowinski K, Jensen S, Lundahl G, et al. Changes in ventricular repolarization during percutaneous transluminal coronary angioplasty in humans assessed by QT interval, QT dispersion and T vector loop morphology. ***J Intern Med.*** Aug 2000;248(2):126-136.

41. Rubulis A, Jensen J, Lundahl G, et al. T vector and loop characteristics in coronary artery disease and during acute ischemia. ***Heart Rhythm.*** Sep 2004;1(3):317-325.

42. Fayn J, Robel P, Arnaud P. A new methodology for optimal comparison of serial vectorcardiograms. ***Computers in Cardiology.*** 1983:467-470.

43. Badilini F, Maison Blanche P, Fayn J, et al. Relationship Between 12-Lead ECG QT Dispersion And 3D-ECG Repolarization Loop. ***Computers in Cardiology.*** 1995:785-788.

44. Kors JA, van Herpen G, van Bemmel JH. QT dispersion as an attribute of T-loop morphology. ***Circulation.*** Mar 23 1999;99(11):1458-1463.

45. Janse MJ, van der Steen AB, van Dam RT. Refractory period of the dog's ventricular myocardium following sudden changes in frequency. ***Circ Res.*** Feb 1969;24(2):251-262.

46. Seed WA, Noble MI, Oldershaw P, et al. Relation of human cardiac action potential duration to the interval between beats: implications for the validity of rate corrected QT interval (QTc). ***Br Heart J.*** Jan 1987;57(1):32-37.

47. Lepeschkin E, Surawicz B. The measurement of the Q-T interval of the electrocardiogram. ***Circulation.*** Sep 1952;6(3):378-388.

48. Poelzing S, Dikshteyn M, Rosenbaum DS. Transmural conduction is not a two-way street. ***J Cardiovasc Electrophysiol.*** Apr 2005;16(4):455.

49. Poelzing S, Akar FG, Baron E, et al. Heterogeneous connexin43 expression produces electrophysiological heterogeneities across ventricular wall. ***Am J Physiol Heart Circ Physiol.*** May 2004;286(5):H2001-2009.

50. Plotnikov AN, Shvilkin A, Xiong W, et al. Interactions between antiarrhythmic drugs and cardiac memory. ***Cardiovasc Res.*** May 2001;50(2):335-344.

51. Yu H, McKinnon D, Dixon JE, et al. Transient outward current, Ito1, is altered in cardiac memory. ***Circulation.*** Apr 13 1999;99(14):1898-1905.

52. Costard-Jackle A, Goetsch B, Antz M, et al. Slow and long-lasting modulation of myocardial repolarization produced by ectopic activation in isolated rabbit hearts. Evidence for cardiac "memory". ***Circulation.*** Nov 1989;80(5):1412-1420.

53. McAreavey D, Fananapazir L. Altered cardiac hemodynamic and electrical state in normal sinus rhythm after chronic dual-chamber pacing for relief of left ventricular outflow obstruction in hypertrophic cardiomyopathy. ***Am J Cardiol.*** Sep 1 1992;70(6):651-656.

54. Tomaselli GF, Marban E. Electrophysiological remodeling in hypertrophy and heart failure. ***Cardiovasc Res.*** May 1999;42(2):270-283.

55. Herweg B, Fisher JD, Ilercil A, et al. Cardiac memory after radiofrequency ablation of accessory pathways: the post-ablation T wave does not forget the pre-excited QRS. ***J Interv Card Electrophysiol.*** Oct 1999;3(3):263-272.

56. Yanagawa T, Hirai M, Hayashi H, et al. QRST time integral values in 12-lead electrocardiograms before and after radiofrequency catheter ablation in patients with Wolff-Parkinson-White syndrome. ***J Am Coll Cardiol.*** Jun 1995;25(7):1584-1590.

57. Hirai M, Tsuboi N, Hayashi H, et al. Body surface distribution of abnormally low QRST areas in patients with Wolff-Parkinson-White syndrome. Evidence for continuation of repolarization abnormalities before and after catheter ablation. ***Circulation.*** Dec 1993;88(6):2674-2684.

58. Sugino M, Inden Y, Sawada T, et al. Comparison of vectorcardiographic and 12-lead electrocardiographic detections of abnormalities in repolarization properties due to preexcitation in patients with Wolff-Parkinson-White syndrome: proposal of a novel concept of a "remodeling gradient". ***Jpn Heart J.*** May 2000;41(3):295-312.

59. Sawada K, Hirai M, Hayashi H, et al. Spatial ventricular gradient in patients with Wolff-Parkinson-White syndrome in comparison with normal subjects: vectorcardiographic evidence for significant repolarization changes due to preexcitation. ***Intern Med.*** Aug 1995;34(8):738-743.

60. Maison-Blanche P, Badilini F, Fayn J, et al. ***QT dispersion: methodology and clinical significance.*** *In: Olsson S B, Yuan S, Amlie J, eds. Dispersion of ventricular repolarization: State of the art.* Armonk, NY: Futura Publishing Company, Inc.; 2000:41-58.

61. Nowinski K, Bergfeldt L. "Normal" response of the QT interval and QT dispersion following intravenous injection of the sodium channel blocker disopyramide: methodological aspects. ***Cardiovasc Drugs Ther.*** Aug 1995;9(4):573-580.

62. Kors JA, de Bruyne MC, Hoes AW, et al. T-loop morphology as a marker of cardiac events in the elderly. ***J Electrocardiol.*** 1998;31 Suppl:54-59.

63. Akahoshi M, Hirai M, Inden Y, et al. Body-surface distribution of changes in activation-recovery intervals before and after catheter ablation in patients with Wolff-Parkinson-White syndrome: clinical evidence for ventricular 'electrical remodeling' with prolongation of action-potential duration over a preexcited area. ***Circulation.*** Sep 2 1997;96(5):1566-1574.

64. Inden Y, Hirai M, Takada Y, et al. Prolongation of activation-recovery interval over a preexcited region before and after catheter ablation in patients with Wolff-Parkinson-White syndrome. ***J Cardiovasc Electrophysiol.*** Aug 2001;12(8):939-945.

65. Rosen MR. What is cardiac memory? ***J Cardiovasc Electrophysiol.*** Nov 2000;11(11):1289-1293.

66. Prinzen FW, Augustijn CH, Arts T, et al. Redistribution of myocardial fiber strain and blood flow by asynchronous activation. ***Am J Physiol.*** Aug 1990;259(2 Pt 2):H300-308.

67. Prinzen FW, Hunter WC, Wyman BT, et al. Mapping of regional myocardial strain and work during ventricular pacing: experimental study using magnetic resonance imaging tagging. ***J Am Coll Cardiol.*** May 1999;33(6):1735-1742.

68. Sadoshima J, Izumo S. Mechanical stretch rapidly activates multiple signal transduction pathways in cardiac myocytes: potential involvement of an autocrine/paracrine mechanism. ***Embo J.*** Apr 1993;12(4):1681-1692.

69. Sadoshima J, Izumo S. Molecular characterization of angiotensin II--induced hypertrophy of cardiac myocytes and hyperplasia of cardiac fibroblasts. Critical role of the AT1 receptor subtype. ***Circ Res.*** Sep 1993;73(3):413-423.

70. Yu H, Gao J, Wang H, et al. Effects of the renin-angiotensin system on the current I(to) in epicardial and endocardial ventricular myocytes from the canine heart. ***Circ Res.*** May 26 2000;86(10):1062-1068.

71. Plotnikov AN, Sosunov EA, Patberg KW, et al. Cardiac memory evolves with age in association with development of the transient outward current. ***Circulation.*** Aug 3 2004;110(5):489-495.

72. Plotnikov AN, Yu H, Geller JC, et al. Role of L-type calcium channels in pacing-induced short-term and long-term cardiac memory in canine heart. ***Circulation.*** Jun 10 2003;107(22):2844-2849.

73. Patel PM, Plotnikov A, Kanagaratnam P, et al. Altering ventricular activation remodels gap junction distribution in canine heart. ***J Cardiovasc Electrophysiol.*** May 2001;12(5):570-577.

74. Patel PM, Hussain W, Linde C, et al. Pacing increases Connexin43 expression in patients with hypertrophic obstructive cardiomyopathy. ***Heart Rhythm.*** 2004;1(1):S22.

75. Patberg KW, Shvilkin A, Plotnikov AN, et al. Cardiac memory: mechanisms and clinical implications. ***Heart Rhythm.*** Dec 2005;2(12):1376-1382.

76. Shvilkin A, Ho KK, Rosen MR, et al. T-vector direction differentiates postpacing from ischemic T-wave inversion in precordial leads. ***Circulation.*** Mar 1 2005;111(8):969-974.

77. Sweeney MO, Hellkamp AS, Ellenbogen KA, et al. Adverse effect of ventricular pacing on heart failure and atrial fibrillation among patients with normal baseline QRS duration in a clinical trial of pacemaker therapy for sinus node dysfunction. ***Circulation.*** Jun 17 2003;107(23):2932-2937.

78. Wilkoff BL, Cook JR, Epstein AE, et al. Dual-chamber pacing or ventricular back-up pacing in patients with an implantable defibrillator: the Dual Chamber and VVI Implantable Defibrillator (DAVID) Trial. ***Jama.*** Dec 25 2002;288(24):3115-3123.

79. Kostin S, Rieger M, Dammer S, et al. Gap junction remodeling and altered connexin43 expression in the failing human heart. ***Mol Cell Biochem.*** Jan 2003;242(1-2):135-144.

80. Pak PH, Nuss HB, Tunin RS, et al. Repolarization abnormalities, arrhythmia and sudden death in canine tachycardia-induced cardiomyopathy. ***J Am Coll Cardiol.*** Aug 1997;30(2):576-584.

81. Darpö B. Spectrum of drugs prolonging QT interval and the incidence of torsade de pointes. ***Eur Heart J.*** 2001;3 (Suppl. K): K70-K80.

82. Nowinski K, Gadler F, Jensen-Urstad M, et al. Transient proarrhythmic state following atrioventricular junctional radiofrequency ablation. ***Pacing Clin Electrophysiol.*** Mar 2002;25(3):291-299.

83. Nowinski K, Gadler F, Jensen-Urstad M, et al. Transient proarrhythmic state following atrioventricular junction radiofrequency ablation: pathophysiologic mechanisms and recommendations for management. ***Am J Med.*** Nov 2002;113(7):596-602.

84. Roden DM. Drug-induced prolongation of the QT interval. ***N Engl J Med.*** Mar 4 2004;350(10):1013-1022.

Appendix 1. Programmed rates, AV-intervals, percent pacing according to the pacemaker log at each follow-up and rates during each VCG-recording for the 14 long-term (LT) and 6 short-term (ST) study patients.

Patient	Rates Lower / Upper (BPM)	AV-interval paced / sensed (ms)	% pacing during follow-up (upper) VCG rate (lower) (BPM) pre/d1/w1/w2/w3/w4/w5/w6/w7/w8/w9	AV-intervals last visit paced / sensed (ms)	% pacing last visit (upper) VCG rate (lower) (BPM)
LT01	70-60 / 120	100 / 50	0/100/100/100/100/100/100/100/100~ 54/69/60/60/69/69/69/69/69~	180 / 140	100 60
LT02[a]	70-50 / 120-150	150 / 120	0/100/100/100/100/99/96/100~ 73/82/68/65/77/65/68/70~	150 / 140	77[b] 84
LT03[a]	45-50 / 120-140	150 / 120	0/100/100/99/100/100/NA/100/99~ 48/45/45/45/45/44/NA/44/49~	230 / 200	78 77
LT04	40 / 160	150 / 50	0/100/100/100/100/100/100/100/100~ 58/60/54/62/62/85/65/68~	120 / 90	51 75
LT05	60 / 150	150 / 120	0/100/100/100/100/100/100/100/100~ 44/60/60/66/61/61/61/60/67~	310 /NA[c]	0 60
LT06	60 / 130	80 / 60	0/NA/100/100/100/100/100/100/100~ 51/NA/60/60/60/60/60/60~	180 / 150	3 60
LT07	70 / 140-120	150 / 120	0/NA/99/99/99/99/100~ 69/NA/72/72/67/68/64~	230 /180	44 70
LT08	60 / 120-160	110 / 90	0/NA/100[d]/91/86[b]/91/97/87[bd]/96~ 54/NA/101[d]/60/60[b]/60/60/103[bd]/60~	150 / 120	79 60
LT09			Excluded due to ventricu- lar lead dislocation		
LT10	60 / 120-160	110 / 80	0/100/100/100/100[e]/100/100/100/100/98/100~ 69/60/60/60/60[e]/67/65/60/60/60/60~	150 / 120	100 60
LT11	60 / 120	60 / 60	0/NA/100/100/NA/100/100/100~ 46/NA/60/60/60/61/61/61~	150 / 120	63 60
LT12	60-75 / 120	120 / 100	0/99/94[d]/93/100/100/100/100/100~ 59/77/100[d]/60/76/75/75/75/75~	220 / 190	38 75
LT13	60 / 120	120 / 90	0/NA/97/97/96/92/93/95/96~ 63/NA/98/98/84/118/87/87/75~	150 / 120	94 68
LT14[a]	60 / 120	150 / 120	0/100/100/100/100/100/100/100/100~ 78/79/66/65/61/65/64/61~	150 / 120	100 59
LT15	60 / 130-125	130 / 100	0/100/100/100/100/NA/100/100/100/100~ 72/72/64/62/61/NA/62/72/67/64~	250 / 200	40 64

Patient	Rates Lower / Upper (BPM)	AV-interval paced / sensed (ms)	% pacing during follow-up (upper) VCG rate (lower) (BPM) pre/d1/d2/d3/d4/d5/d6/d7/d8/d10	AV-interval last visit paced / sensed (ms)	% pacing last visit (upper) VCG rate (lower) (BPM)
ST01	60 / 125	120 / 100	0/62/96/92/98/87/NA/99~ 49/60/60/60/63/60/NA/60~	NA	NA
ST02	70 / 130	120 / 100	0/100/100/18[bd]/0[bd]/1[bd]/3[bd]/3[bd]~ 43/69/69/87[bd]/104[bd]/83[bd]/80[bd]/89[bd]~	NA	NA
ST03	60 / 130	120-110 / 100	0/100/100/100/100/NA/100/100~ 57/60/60/60/60/NA/60/60~	NA	NA
ST04[a]	50 / 130-120	150 / 120	0/100/100/100/100/100/100/100/NA/100~ 41/54/53/58/57/53/50/49/NA/49~	NA	NA
ST05[a]	60 / 140	150 / 120	0/100/100/100/100/100/100/100/100~ 41/58/60/60/60/60/60/60/60~	NA	NA
ST06	60 / 170	120 / 100	0/100/100/100/100/100/100/100/100~ 58/65/74/71/84/69/66/93/71~	NA	NA

BPM = beats per minute
pre = baseline, sinus rhythm before pacemaker implantation
d1 = 1 day after pacemaker implantation, etc.
w1 = 1 week after pacemaker implantation, etc.
Rate “70-60” and AV-interval “120-110”means reprogramming from 70 to 60 BPM and from 120 to 110 ms, resp.
~ end of follow-up
a AV-block I prior to pacemaker implantation
b Mode-switch due to atrial fbrillation >20% of the time since last follow-up
c DDI-mode
d Atrial fibrillation at follow-up
e Loss of capture